SLAC PROPOSAL NO. E-131
Received Dec. 27, 1976

A SLAC STREAMER CHAMBER PROPOSAL TO STUDY PRODUCTION MECHANISMS FOR IDEALLY MIXED $s\bar{s}$ SYSTEMS IN π^+p INTERACTION AT 15 GeV/c

F.T. Dao, W.A. Mann, R.H. Milburn, W.P. Oliver,
J. Schneps and R.K. Thornton
Tufts University
and
J. Hylen and Z. Ming Ma
Michigan State University
and
J.M. Bishop, N.N. Biswas, N.M. Cason, V.P. Kenney and
W.D. Shephard
University of Notre Dame

TABLE OF CONTENTS

I PHYSICS MOTIVATION

(a) Production Mechanisms for Ideally Mixed $s\bar{s}$ Systems

Since the discovery of ψ/J (3095) at BNL[1] and SLAC[2] there has been considerable evidence supporting the assumption of a fourth quark, called the charmed quark (c for short). By now, there is strong credibility that the ψ/J (3095) is an orthocharmonium state[3] with other higher mass enhancements being identified as excited states in this $c\bar{c}$ bound state picture. To complete this picture, it is absolutely necessary[4] that mesons and baryons with a non-zero charm quantum number exist. Experimental searches for these charmed particles have been largely in e^+e^- and nucleon-nucleon interactions. Recently, a narrow enhancement has been reported by the LBL-SLAC collaboration using SPEAR.[5,6] The structure is observed at a mass of $1.865 \pm .015$ GeV/c^2 and has a full width less than 40 MeV/c^2. Neutral decay modes of this particle have been seen in the $k^{\pm}\pi^{\mp}$ and $k^{\pm}\pi^{\mp}\pi^{+}\pi^{-}$ states[5] and charged signals in the $k^{\pm}\pi^{\mp}\pi^{\mp}$ modes are also reported.[6] If these effects are indeed due to charmed particles, one would expect to detect copious production of these states in hadronic interactions. To date no convincing evidence has turned up in hadronic interaction[7-12] at a level of $\sigma.B > 40$ nb[13] where B is the branching ratio.

Since $\phi(1019)$ is a nearly ideally mixed $s\bar{s}$ state, it is very likely that production mechanisms for $\phi(1019)$ and $\psi/J(3095)$ share many common features. Therefore, a rigorous and high statistics study of the production dynamics of $\phi(1019)$ and its relation to the production of strange particles may shed light on the production mechanisms of $\psi/J(3095)$ and the charmed particles. Empirical rules, such as Zweig's rule,

may be applicable to $\psi/J(3095)$. Although Zweig's rule was proposed to explain the suppression of ϕ decay into the $\rho\pi$ state, it has been used extensively to interpret ϕ and J/ψ production data. Although applicability of Zweig's Rule to production dynamics has not been unambiguously demonstrated, available experimental evidence seems to lend qualitative support to such a notion. For example, in the reaction

$$\pi^- p \to \phi n \tag{1}$$

Ayres[14] observed that the reaction is suppressed relative to the reaction

$$\pi^- p \to \rho n \tag{2}$$

by a factor of 3.6×10^{-3} from threshold to 6 GeV/c. At 19 GeV/c, the Omega Spectrometer group found[15] a suppression factor of $(5^{+5}_{-2}) \times 10^{-3}$ against the reaction

$$\pi^- p \to \phi\, \pi^+\pi^-\pi^- p \tag{3}$$

relative to the reaction

$$\pi^- p \to \omega\pi^+\pi^-\pi^- p \tag{4}$$

using a total of 44±10 events from reaction (3). These results are consistent with Zweig's Rule. Except for the ϕ meson, none of the other participants in the reactions (1) and (3) is known to carry a significant amount of the strange quark (s) in its wave function. Therefore, the s and $\bar{s}$ quark lines from the ϕ meson must terminate on themselves. And this is forbidden by Zweig's Rule. Furthermore, a comparison of the production cross sections for reactions (1) and (2) lends support to the notion that these two reactions may indeed be governed by different mechanisms. Referring to Figure 1, the cross section for ϕ production

exhibit a very steep drop-off ($\sigma \sim P_L^{-3.5}$) following a rapid rise from threshold. This is characteristic of Fermi's statistical model or a Regge cut model. In comparison, the ρ production cross-sections fall slowly with energy ($\sigma \sim P_L^{-1.89 \pm .09}$).

Suggestions have been made [16] that Zweig's rule is strictly observed for ideally mixed vector and tensor meson states. The apparent violations such as reaction (1) are due to the mixing effect in the physical particles. It therefore, follows that the cross section ratio, R, is given by

$$R \equiv \frac{\sigma(\pi^- p \to \phi n)}{\sigma(\pi^- p \to \omega n)} = g^2_{\phi\rho\pi}/g^2_{\omega\rho\pi} \simeq 10^{-2} \qquad (5)$$

The cross section ratio is expected to be a constant. The cross sections for the reactions

$$\pi^- p \to \omega n \qquad (6)$$

and

$$\pi^+ n \to \omega p \qquad (7)$$

are shown in Figure 1. As may be seen,the energy dependency for reactions (6) and (7) is very similar to that of reaction (2) and the cross section fall-off is milder than that for reaction (1). Similar results have been reported by a Liverpoool group[17] in a comparison of the reactions

$$\bar{p}p \to K^+K^-\omega^o \qquad (8)$$

and

$$\bar{p}p \to K^+K^-\phi \qquad (9)$$

at 3.6 GeV/c. Here the observed rate based on 12 events for reaction (9) is an order of magnitude higher than would be expected from the measured rate for reaction (8) and the 10^{-2} ratio of equation (5).

Recently, a theoretical attempt to understand reaction (1) in terms of a double Regge pole exchange picture was advanced by Berger and Sorensen.[18] Figure 2(a) shows the proposed exchange mechanism. The precipitous drop-off in the production cross sections is explained in terms of a cancellation effect by K (890) and K (1420) in the intermediate state. Although the model can account for the shape of the cross section drop-off, it fails to predict its experimental magnitude by a factor of 3. In addition, the model predicts a turn over in the t-distribution which is not observed experimentally.

It was first pointed out by Sivers[19] that one might expect to observe copious Zweig's Rule allowed production of ϕ mesons with a pair of strange particles (Figure 2(b)). An example of this mechanism (Figure 2(c)) would be

$$\pi^+ p \to K^+ \phi \Sigma^+ \tag{10}$$

where the s and $\bar{s}$ quarks from the ϕ meson terminate on the neighboring K^+ and Σ^+ respectively. Experimental data relevant to this question are quite limited. In $\bar{p}p$ interaction at 3.6 GeV/c, the cross section ratio is reported[17] to be

$$\sigma(\bar{p}p \to \phi\pi^+\pi^-)/\sigma(\bar{p}p \to \phi K^+K^-) = 0.7 \pm .3 \tag{11}$$

based upon a total of 24 ± 4 ϕ events. Data from the OMEGA Spectrometer Group indicated[15] that in the π^-p interaction at 19 GeV/c, the cross section ratio is

$$\sigma(\pi^-p \to \phi\pi^+\pi^-\pi^-p)/\sigma(\pi^-p \to \phi K^+K^-\pi^-p) = 1.7\ ^{+.9}_{-.5} \tag{12}$$

for $x > 0.3$ based on a total of 90 ϕ events. In both cases, the ratios are consistent with being one. However, in both experiments, ϕ events represent a larger fraction of the final states when an additional pair of

kaons are involved.

H. Lipkin[16] has argued that the proper interpretation for experimental data such as (11) and (12) is complicated by the fact that it is difficult to produce a kaon pair in any reaction. The cross section ratios (11) and (12) merely indicate the relative difficulties for Zweig's rule violations as compared with producing an extra pair of charged kaons. Available data, therefore, seem to support the notion that these two processes are comparable in magnitude.

Using a quark fusion model, Donnachie and Landshoff[20] argued that the conjoint-type of production may be suppressed by the final state interaction similar to the quark confinement problem. Such a mechanism may be responsible for the null results[21] in the search for the conjoint production of charmed particles with $\psi/J(3095)$ at 300 GeV/c. It may also provide a frame work for understanding the cross section suppression associated with the production of a kaon pair.

In summary, experimental facts on Zweig's rule are very scarce and our understanding of the dynamic origin of Zweig's rule is very limited. A careful study of ϕ producing reactions may not only shed light on the mechanism for producing a bound state of a pair of identical quarks, such as ϕ, f' (1520), ψ/J (3095), etc. in hadronic interaction, but also can provide a basis for understanding the dynamic origin of Zweig's rule. Furthermore, since ϕ production cross sections are of the order of 10^2 μb, it makes sense to test dynamic models such as the conjoint production pictures of Sivers (e.g. ϕ production in association with a pair of strange particles and ψ/J (3095) production in association with a pair of charmed particles) using the ϕ-meson before embarking on a massive search for charmed particles using ψ/J or ψ' mesons.

A survey of currently existing data indicates that except for reaction (1), data are not available for a systematic study of exclusive ϕ production reactions where Zweig's rule may play an important role. We propose to study the production mechanisms for ϕ-meson at a level of 2.54 events/nb times the acceptance of the system. The proposed trigger reaction is

$$\pi^+ p \rightarrow K^- + X \qquad (12)$$

at 15 GeV/c. The rationale for the choice of the reaction is discussed in Section I(c). The details of triggering efficiency and the expected yield of this experiment are discussed in Section III.

(b) Search for New High Mass $K\bar{K}$ States

An effective K^- trigger will also make possible a high statistics search for new high mass $K\bar{K}$ states. One such state that is of particular interest here is the ϕ', the missing member of the $J^P = 3^-$ nonet.[22] It is expected that ϕ should have a mass between 1800 and 1900 MeV/c^2 and has an appreciable decay rate into $K\bar{K}$ states. The triggering efficiency as a function of the $K\bar{K}$ mass is given in Figure 3(a). Here the $K\bar{K}$ pair is assumed to be isotropicly produced. At a mass of 1800 MeV/c^2, it is expected that a 100 event/μb sensitivity can be achieved.

(c) Rationale for the Trigger Reaction $\pi^+ p \to K^- + X$

To trigger on the ϕ production using its decay mode

$$\phi \to K^+K^- \tag{13}$$

one can use either a K^+ or a K^- as a signature. It is well known that the principle source for K^+ particles is associated production. Although no bubble chamber data exist on the total associated production cross section involving a K^+, Bosetti et al[24] estimated that the inclusive K^+Y cross section from $\pi^+ p$ at 16 GeV/c is 936 ± 90 μb. Here, an assumption was made that the production of more than two strange particles and the production of $|S| > 1$ strange particle are negligible. To avoid this very sizeable event rate, we decided on a K^- trigger.

Due to the strangeness conservation, a K^- must be accompanied by a K^+/K° or a $\bar{\Lambda}/\bar{\Sigma}$,N pair. Available data from a bubble chamber experiment[23] indicate that cross sections from the $K^-N\bar{\Lambda}/\bar{\Sigma}$ states are small (< 50 μb). The contribution from the K^-K° state is expected to be considerable. For example, both A_2° or A_2^- production can feed the K^- trigger rate. Since the A_2 production can proceed via vector or tensor meson exchange, these processes are expected to be peripheral, whereas the ϕ mesons tend to be produced in the central region. Since the K^- is composed of $\bar{s}d$, one would expect its production be suppressed in the forward region for a π^+ beam ($u\bar{d}$) as compared with a π^- beam ($\bar{u}d$). The number of available channels for producing a K^-K° state is also reduced considerably for a π^+p initial state as compared to a π^-p interaction by charge conservation. The above factors persuaded us to decide in favor of a π^+ beam. The cross section for reaction 12 is estimated to be 0.57 ± .19 mb near 15 GeV/c and is discussed in Appendix I. The inclusive ϕ cross section is estimated to be

$90 \pm 13\mu b$ for $x > 0$. This comes from an comparison of inclusive data[25,26] from $\pi^+ p$ at 150 GeV/c and $\pi^- p$ at 19 GeV/c. The details are presented in Appendix II. Assuming that K^- production is symmetric with respect to $x = 0$ in the c.m., one expects that 16 % of the K^- cross section invloves a ϕ-meson.

II EXPERIMENTAL SETUP

The proposed set up is shown in Figure 4. A 15 GeV/c π^+ beam is incident upon a 60 cm liquid hydrogen target placed at the center of the streamer chamber. The K^- trigger is shown to the right of the beam line. Three sets of vertical picket fence counters are placed at 2,3 and 4 meters downstream of the target. These are designated as V_{1i}, V_{2i}, and V_{3i} ($i = 1,2,...20$). The first array is composed of 20 counters, each measuring 3 cm wide by 40 cm high. The left edge of V_{11} is placed on the center line of the streamer chamber. Counters of the second array are 4.5 cm wide by 60 cm high and are placed 3 cm to the right of the center line. The third array is shifted 6 cm to the right and each element measures 6 cm by 80 cm.

Immediately downstream of the V_{3i} array is a 10-cell isobutane threshold Čerenkov counter. The counter is 2 m long and has 10 mirrors at the back in the form of a 2x5 matrix convering an area of 2 m wide by 1.25 m high. It will be operated with isobutane gas at atmospheric pressure and will have better than 99.9% efficiency for pions of 4 GeV/c or above. Detailed design considerations are given in Appendix III. A fourth array of 20 counters V_{4i}, ($i = 1,2,...20$) are deployed immediately behind the Čerenkov counter. Each counter measures 12.5 cm wide by 1.25 m high.

To the left of the streamer chamber center line is the K^+ tagging system. It is composed of a 1 m long threshold Čerenkov counter sandwiched in between two planes of proportional wire chambers. The Čerenkov counter is of a similar design except for a shorter radiator length, as that used in the K^- arm. It has 6 mirrors at the back of the counter in the form of a 2x3 matrix. The entrance and exit windows of the Čerenkov counter each cover an area of 1.2 m wide by 1.25 m high as are the PWC's.

The right-hand side edge of the K^+ tagging system will be displaced 20 cm to the right of the streamer chamber center line. The entrance window will be at 3 meter downstream from the center of the target.

In this experiment, the trigger will be

$$\pi^+ \cdot \sum_i V_{1i} \cdot V_{2i} \cdot V_{3i} \cdot V_{4i} \cdot \overline{\overset{V}{C}_i(K^-)} \qquad (14)$$

For every trigger, the K^+ $\overset{V}{\text{C}}$erenkov Counter pulse height information and the PWC information will be tagged and recorded on magnetic tape for off-line analysis.

III TRIGGER YIELD AND BACKGROUND ESTIMATES

The total π^+p cross section at 15 GeV/c is[23] 24.05 ± .28 mb. A 60 cm long target corresponds to a 5.88% probability that an incident π^+ will interact in the liquid hydrogen. With 8 π^+/pulse, one has 0.47 interaction/pulse. In 300 hours, this experiment will have an equivalent sensitivity of 2.54 interaction/nb at 120 pps.

(a) ϕ-Meson Yields

Figure 3(a) shows the percent acceptance of our system as a function of the K^+K^- mass. The K^- decay loss is already included. At the ϕ mass, the acceptance is 4.85% averaged over the entire x range. This assumes an isotropic production in the c.m. system. On the other hand, if the dynamic features of the ϕ production at 15 GeV/c is the same as that at 150 GeV/c, its differential cross section is given by

$$E\frac{d\sigma}{d\vec{p}} \sim (1-x)^{1.73 \pm .44}\, e^{-(3.61 \pm .40)P_T^2} \qquad (15)$$

the acceptance of our system becomes 8.85% for $x > 0$. The inclusive ϕ cross section for $x > 0$ is estimated in Appendix II to be 90 ± 13 μb. Assuming equation (15) is valid for 15 GeV/c π^+p interaction, we expect to have

$$N_\phi = 90 \times 1/2 \times 8.85\% \times 2.54 \times 10^3 = 1.01 \times 10^4 \text{ events} \qquad (16)$$

An estimated 62.2% of these events or 6.28×10^3 events will have both K^+ and K^- tracks identified in the Čerenkov counters. The x and P_T^2 dependencies of the acceptance are shown in Figure 5.

(b) K^- Yields without a ϕ Meson

Turning to the K^+K^- and K^-K^o system in general, the averaged geometric acceptance for the K^- track is 4.45% for the picket fence logic

$$\pi^+ \cdot \sum_i V_{1i} \cdot V_{2i} \cdot V_{3i} \cdot V_{4i} \qquad (17)$$

The $K\bar{K}$ pair is assumed to be produced isotropically in the c.m. system. Demanding a null signal from the corresponding cell in the Čerenkov counter, the averaged acceptance is reduced to 3.30%. The inclusive K^- cross section is estimated in Appendix I to be 0.57 ± .19 mb. About 2/3 of this cross section is attributed to the K^+K^- state and the remaining 1/3 is due to the K^-K^o state. Therefore, excluding the ϕ production, the inclusive K^- cross section is

$$\sigma_{K^-} = (570 \pm 190) - (90 \pm 13) = 480 \pm 190 \ \mu b \qquad (18)$$

The expected yield is given by

$$N_{K^-} = 480 \times 3.30\% \times 2.54 \times 10^3 = 4.02 \times 10^4 \text{ events} \qquad (19)$$

of this sample, 2.43×10^4 events are due to the K^+K^- states. The remaining 1.59×10^4 events come from the K^-K^o states. Figure 3 shows the probability that a triggered event has its K^+ track identified in the other Čerenkov counter. The probability declines with increasing K^+K^- mass. The missing K^+ remaining at large is either due to its geometry or being below Čerenkov threshold for a π^+. At low K^+K^- mass, these two factors contribute equally to this loss. The averaged K^+ acceptance is 10.0%, therefore, we expect the number of non-ϕ events with both charged kaons identified to be

$$N_{K^+K^-} = 2.43 \times 10^4 \times 10.0\% = 0.24 \times 10^4 \text{ events} \qquad (20)$$

For the K^-K^o states, we have

$$N_{K^-K^o_s} = 1.59 \times 10^4 \times 1/2 \times 68.8\% = 0.55 \times 10^4 \text{ events} \quad (21)$$

for which both kaons are identified.

(c) π^- Background Trigger

Monte Carlo studies using experimental data[23] on

$$\pi^+ p \rightarrow \pi^- + \text{anything} \quad (22)$$

at 15 GeV/c indicate that 13.7% acceptance is expected for π^- based on the picket fence trigger logic (17). The total inclusive π^- cross section is 24.50 ± .34 mb, therefore, without the Čerenkov counter, the expected π^- to K^- ratio would be

$$R(\pi^-/K^-)_{\text{no C}} = 24.50\text{x}13.7\%/[(0.57-0.09)\text{x}4.45\%+0.09\text{x}1/2\text{x}8.85\%] = 132 \quad (23)$$

Using the design specification for the atmospheric pressure isobutane Čerenkov counter as is discussed in Appendix III, the noise to signal ratio is reduced to

$$R(\pi^-/K^-)_{C} = 0.020\% \text{ x } 24.50/[(0.57-0.09)\text{x}3.30+0.09\text{x}1/2\text{x}8.85\%] = 0.25 \quad (24)$$

This corresponds to 12.4K events. Since about 1/3 of this contamination comes from π^- tracks with a momentum slightly above the Čerenkov counter, threshold, it can be removed during the off-line analysis stage by a momentum cut.

(d) Random Veto of K^- Triggers by π^+ or π^-

A proper K^- trigger may be accidentally vetoed by a π^+ or π^- entering the same Čerenkov cell. The probabilities for a π^+ or π^- above threshold hitting a 1.25 m by 2 m area at the mirror plane are 1.5% and 27.3% respectively. Since the inclusive cross sections for π^+ and π^- are

61.34 ± .73 mb and 24.50 ± .34 mb respectively, the averaged number of accidental $\pi^{\pm}$ is given by

$$(61.34 \times 1.5\% + 24.50 \times 27.3\%) / 24.05 = 0.32 \qquad (25)$$

The Čerenkov counter is divided into 5 distinct cells. Assuming that the $\pi^{\pm}$ veto occurs at random, the probability for a lost K^- trigger is 0.32/5 or 6.4%. This factor has been incorporated into all previous calculations.

(e) Random Veto of K^+ Tags by π^+ or π^-

As is discussed in III.D, a proper K^+ tag may be lost due to a π^+ or π^- entering the same Čerenkov cell. These probabilities are calculated to be 26.7% and 1.3% for a π^+ and a π^- respectively. Using information from the PWC's and the 6-cell Čerenkov counter, we expect a random veto probability of 11.6%. This factor is already included in all previous discussions.

(f) Dead Time Consideration

Due to the low trigger rate in this experiment, dead time losses would be minimal. The expected number of triggers is 64.1 K. Allowing for 150 K pictures and 300 millisecond for film advance, the dead time losses amount to 4.17% of the available beam.

(g) Considerations for Alternative Facilities

Since the cross section for inclusive ϕ production at 15 GeV/c is expected to be reasonably high (90 μb for $x > 0$), we have considered the use of the SLAC Hybrid Facility (SHF) for this experiment. In Appendix IV, a careful comparison is made for the demands on the 40" Bubble Chamber Hybrid Facility and the streamer chamber facility for a comparable yield.

We concluded that for this experiment, it is advantageous to use the streamer chamber facility not only for the economy of the linac pulses, but also for a larger x range for the ϕ meson with less π^- contamination in the trigger.

Finally, a summary of the expected sample yield from this experiment is given in Table I.

IV SUMMARY OF REQUEST

1. Beam: π^+ at 15 GeV/c
   a. Momentum and angular dispersions: $\Delta p/p \simeq \pm 3/4\%$ for a beam spot of 6mm FWHM at 30 cm upstream of the center of the streamer chamber. Angular divergence better than $\pm$ 2 mr will be desirable.
   b. Intensity: 8 π^+ per pulse at 120 pps for data run.
2. Machine Time: 300 hours at 120 pps for data run and 500 hours at 10 pps for set up and equipment testing.
3. Liquid Hydrogen Target: A 60 cm long liquid hydrogen target with $\sim$1 cm diameter cross section and its downstream end at the center of the streamer chamber.
4. Fast Electronic Logic: Parts of the fast logic needed in this experiment will be borrowed from the SLAC equipment pool.
5. Computer Time: Processing for up to 2000 streamer chamber events through the SLAC-LBL SIOUX reconstruction-fitting routine is requested. The Minimal Services available on the TRIPLEX systems as is defined in Appendix A of "Interim Policy Statement for Scheduled Experiments," dated March 23, 1976 will be satisfactory.
6. Scanning and Measuring Facilities: Nominal access to the SLAC scanning and measuring facilities for system check out is needed. Measuring for up to 2000 events is requested.
7. Film: up to 150 K triads will be needed.

REFERENCES

1. J.J. Aubert et al., Phys. Rev. Letters 33, 1404 (1974).
2. J.E. Augustin et al., Phys. Rev. Letters 33, 1406 (1974).
3. T. Appelquist, A. De Rujula, H.D. Politzer and S.L. Glashow, Phys. Rev. Letters 34, 365 (1975).
4. M.K. Gaillard, B.W. Lee, and J.L. Rosner, Rev. Mod. Phys. 47, 277 (1975).
5. G. Goldhaber et al., Phys. Rev. Letters 37, 255 (1976)
6. I. Peruzzi et al., Phys. Rev. Letters 37, 569 (1976)
7. J.J. Aubert et al., Phys. Rev. Letters 35, 416 (1975). S.C.C. Ting, Rapporteurs talk given at the EPS International Conference on High Energy Physics at Palermo, Sicily, Italy, June, 1975.
8. V. Hagopian et al., Phys. Rev. Letters 36, 296 (1976).
9. D. Bintinger et al., Phys. Rev. Letters 37, 732 (1976).
10. E.J. Bleser et al., Phys. Rev. Letters 35, 76 (1975).
11. B. Ghidini et al., Nucl. Phys. B 111, 189 (1976).
12. C. Baltay et al., Phys. Rev. Letters 34, 1118 (1975).
13. Z. Ming Ma and B.Y. Oh, Comment on 'Search for More J Particles', to be published in Phys. Rev. Letters.
14. D.S. Ayres, R. Diebold, A.F. Greene, S.L. Kramer, J.S. Levine, A.J. Pawlicki and A.B. Wicklund, Phys. Rev. Letters 32, 1463 (1974).
15. P.L. Woodworth et al., Test Of The Zweig Rule in $\pi^- p$ Interactions at 19 GeV/c, to be published in Nucl. Phys. B.
16. H.J. Lipkin, Phys. Letters 60B, 371 (1976).
17. R.A. Donald et al., Phys. Letters 61B, 210 (1976).

18. E. Berger and C. Sorensen, Phys. Letters 62B, 303 (1976).

19. D. Sivers, Phys. Rev. D11, 3253 (1975).

20. A. Donnachie and P.V. Landshoff, Nucl. Phys. B112, 233 (1976).

21. M. Binkley et al., Phys. Rev. Letters 37, 578 (1976).

22. For a comprehensive review on the current status of SU_3, see Hadrons and SU_3: A Critical Review, by N.P. Samios, M. Goldberg and B.T. Meadows, BNL 17851 (1973).

23. D. Pisello, Ph.D. Dissertation, Columbia University (1976), unpublished.

24. P. Bosetti et al., Nucl. Phys. B94, 21 (1975).

25. K.J. Anderson et al., Phys Rev. Letters 37, 799 (1976).

26. P. Woodworth, CERN Omega Spectrometer Group, private communication.

TABLE I. A SUMMARY OF EXPECTED YIELDS

$K\bar{K}$ States	$\sigma(\mu b)$	K^- Trigger	Both Kaons Identified	π^- Trigger	Total
		5.03×10^4	1.42×10^4	1.24×10^4	6.27×10^4
$\phi \rightarrow K^+K^-$	90±13	1.01×10^4	0.63×10^4		
Other K^+K^- States	290±130	2.43×10^4	0.24×10^4		
All K^-K^o States	190±60	1.59×10^4	0.55×10^4		

FIGURE 1

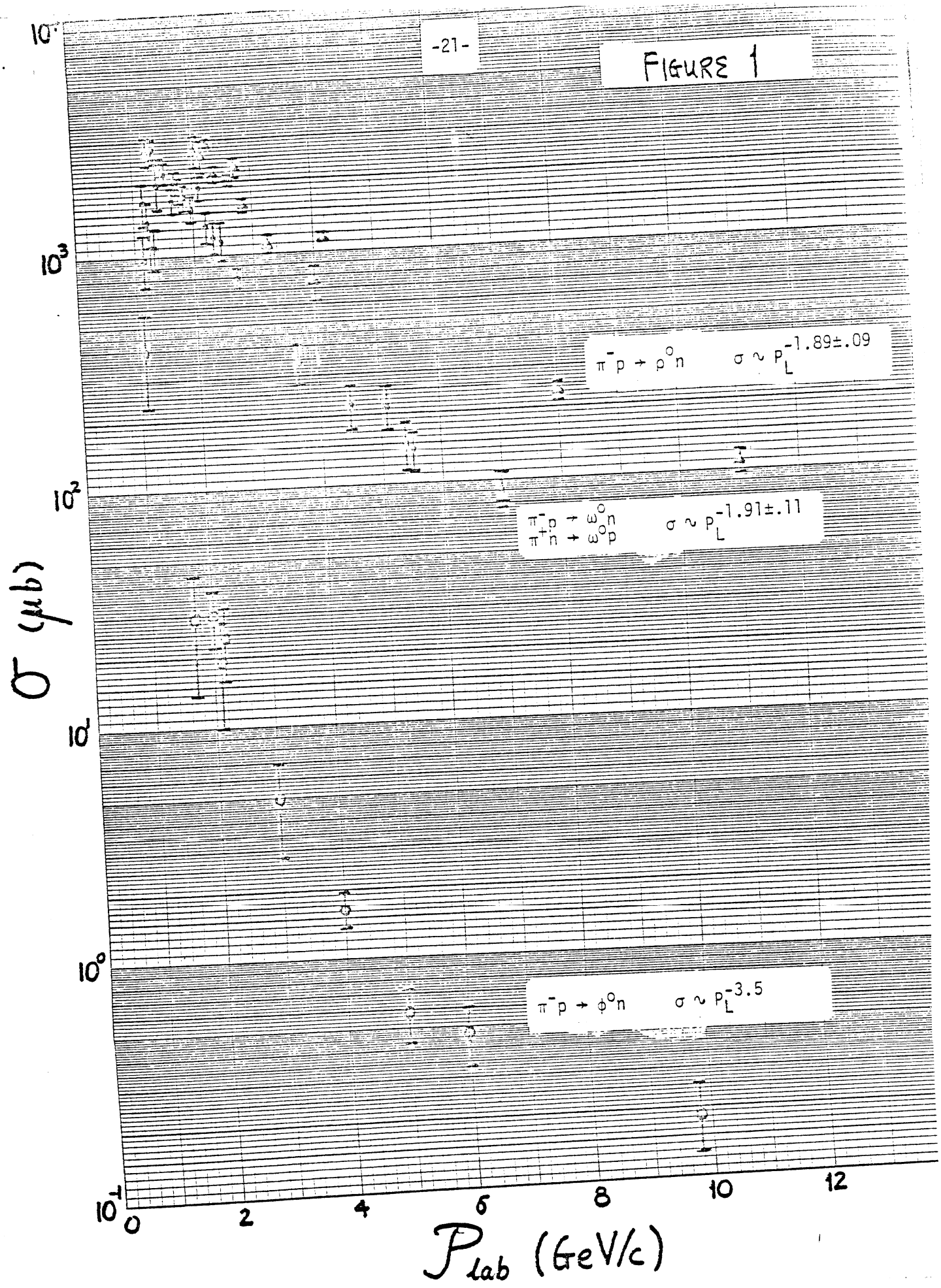
$\pi^- p \to \rho^0 n$ $\sigma \sim P_L^{-1.89\pm.09}$
$\pi^- p \to \omega^0 n$
$\pi^+ n \to \omega^0 p$ $\sigma \sim P_L^{-1.91\pm.11}$
$\pi^- p \to \phi^0 n$ $\sigma \sim P_L^{-3.5}$
σ (μb)
10^3
10^2
10^1
10^0
10^{-1}
0
2
4
6
8
10
12
P_{lab} (GeV/c)

FIGURE 2

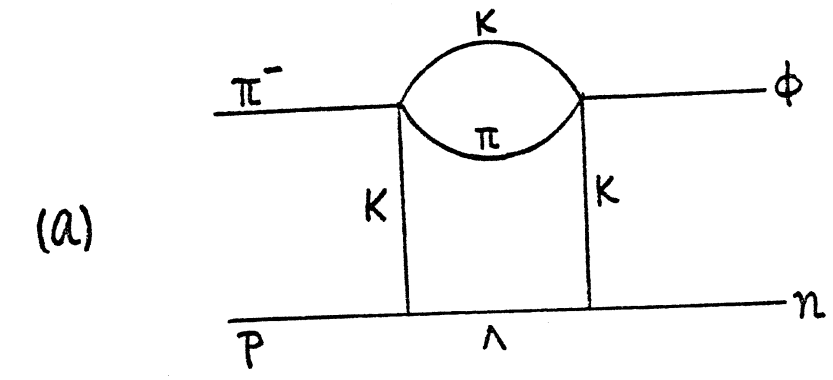

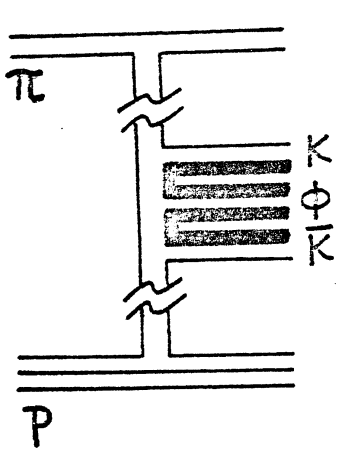

(b)

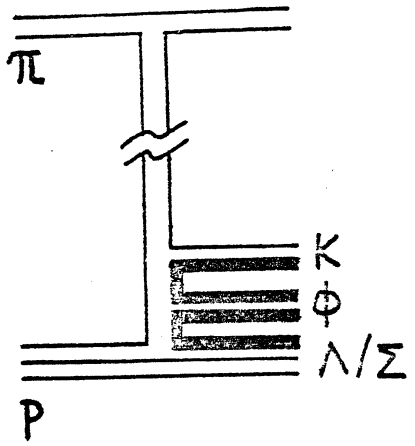

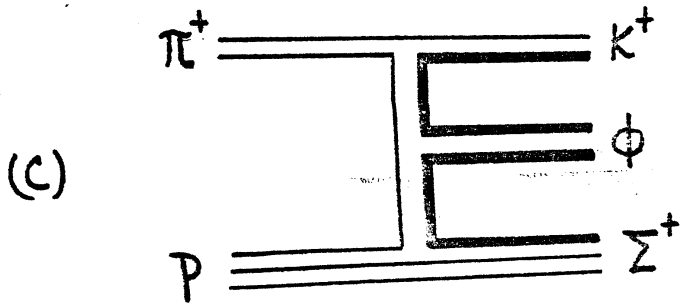

FIGURE 5

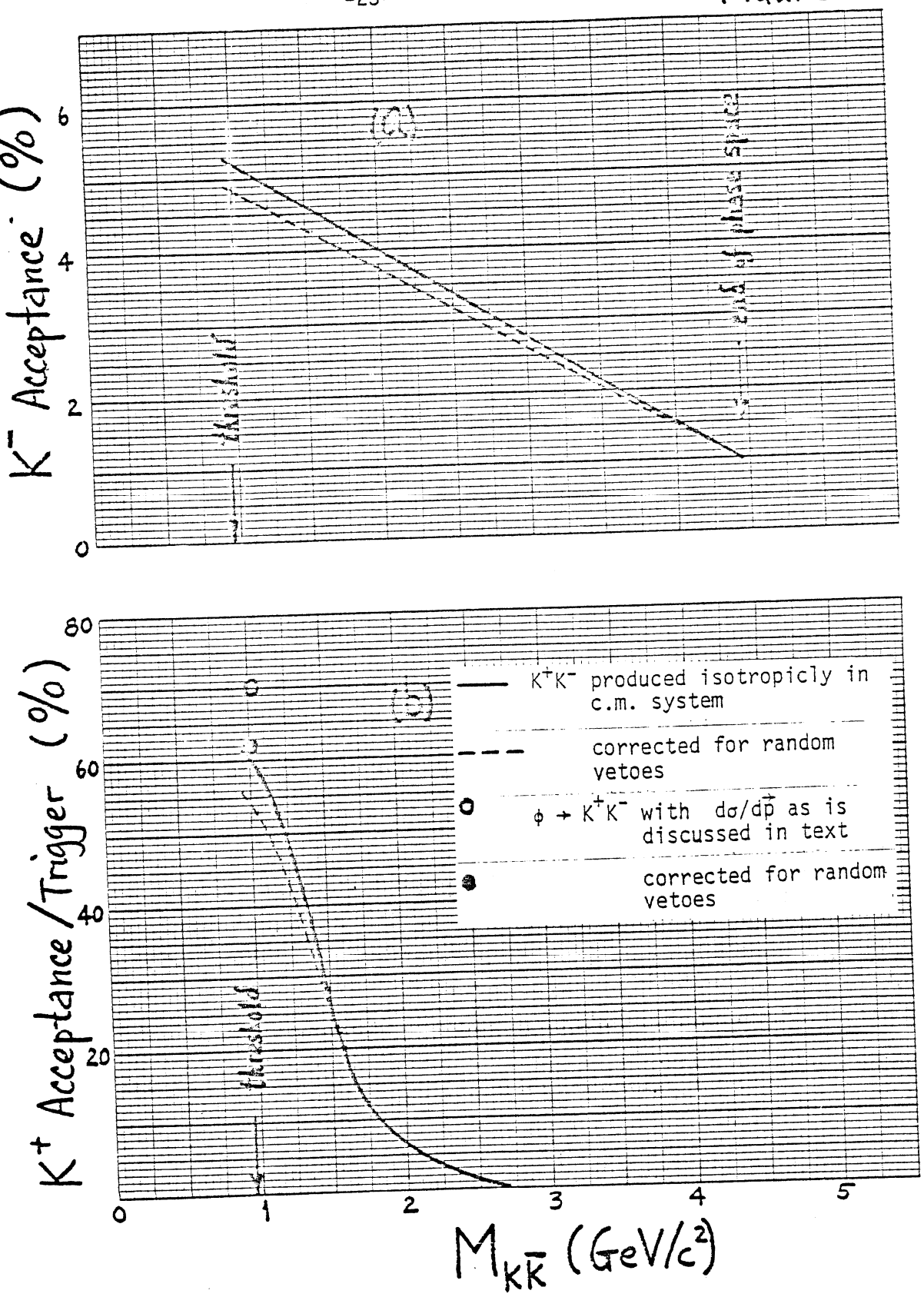
K⁻ Acceptance (%)
6
4
2
0
(a)
threshold
K⁺ Acceptance/Trigger (%)
80
60
40
20
0
(b)
threshold
K⁺K⁻ produced isotropicly in c.m. system
corrected for random vetoes
φ → K⁺K⁻ with dσ/dp⃗ as is discussed in text
corrected for random vetoes
1
2
3
4
5
M_KK̄ (GeV/c²)

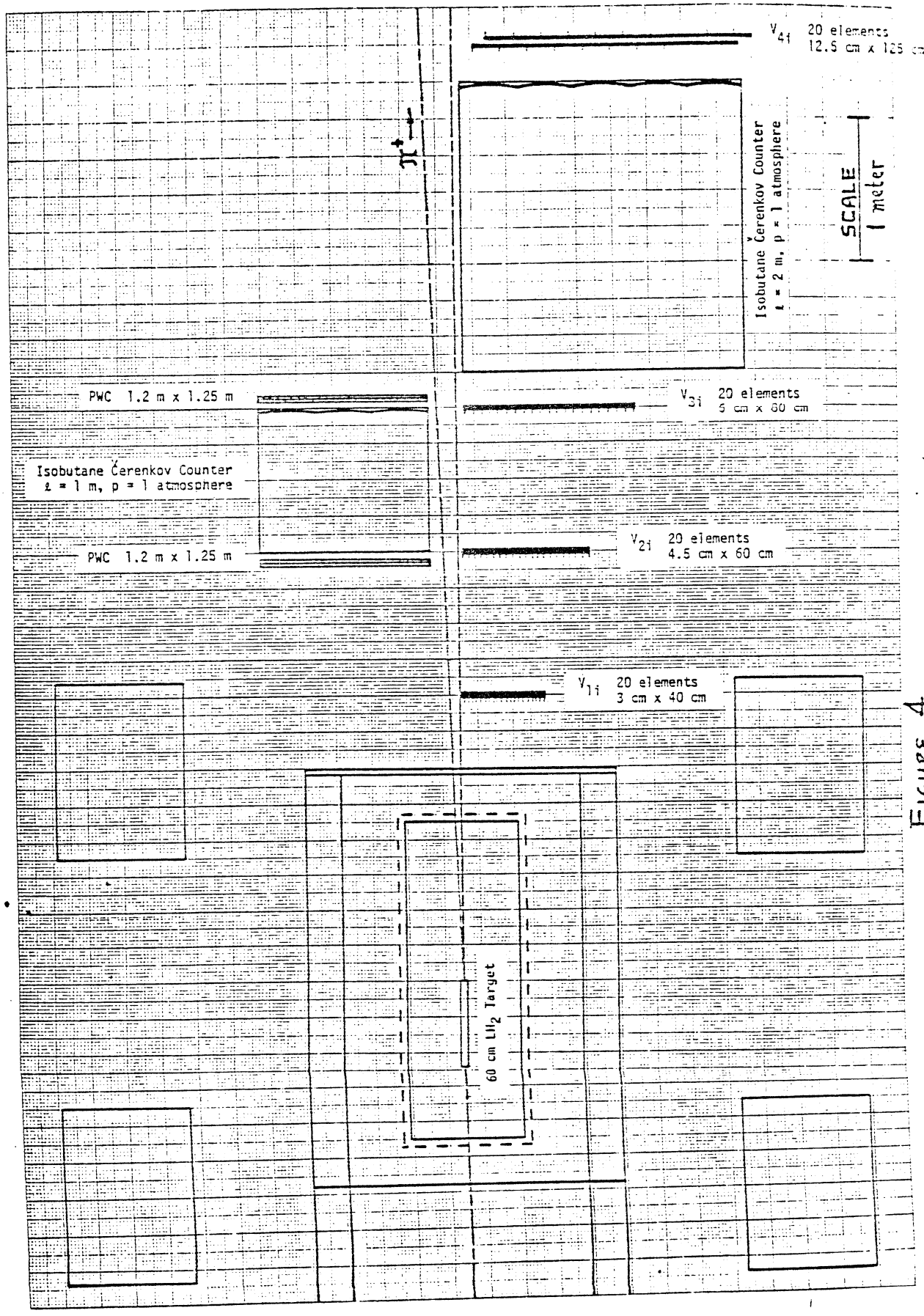
V_{4i} 20 elements
12.5 cm x 125 cm
π^+
Isobutane Čerenkov Counter
ℓ = 2 m, p = 1 atmosphere
SCALE
1 meter
PWC 1.2 m x 1.25 m
V_{3i} 20 elements
5 cm x 60 cm
Isobutane Čerenkov Counter
ℓ = 1 m, p = 1 atmosphere
PWC 1.2 m x 1.25 m
V_{2i} 20 elements
4.5 cm x 60 cm
V_{1i} 20 elements
3 cm x 40 cm
60 cm LH_2 Target

FIGURE 4

FIGURE 5

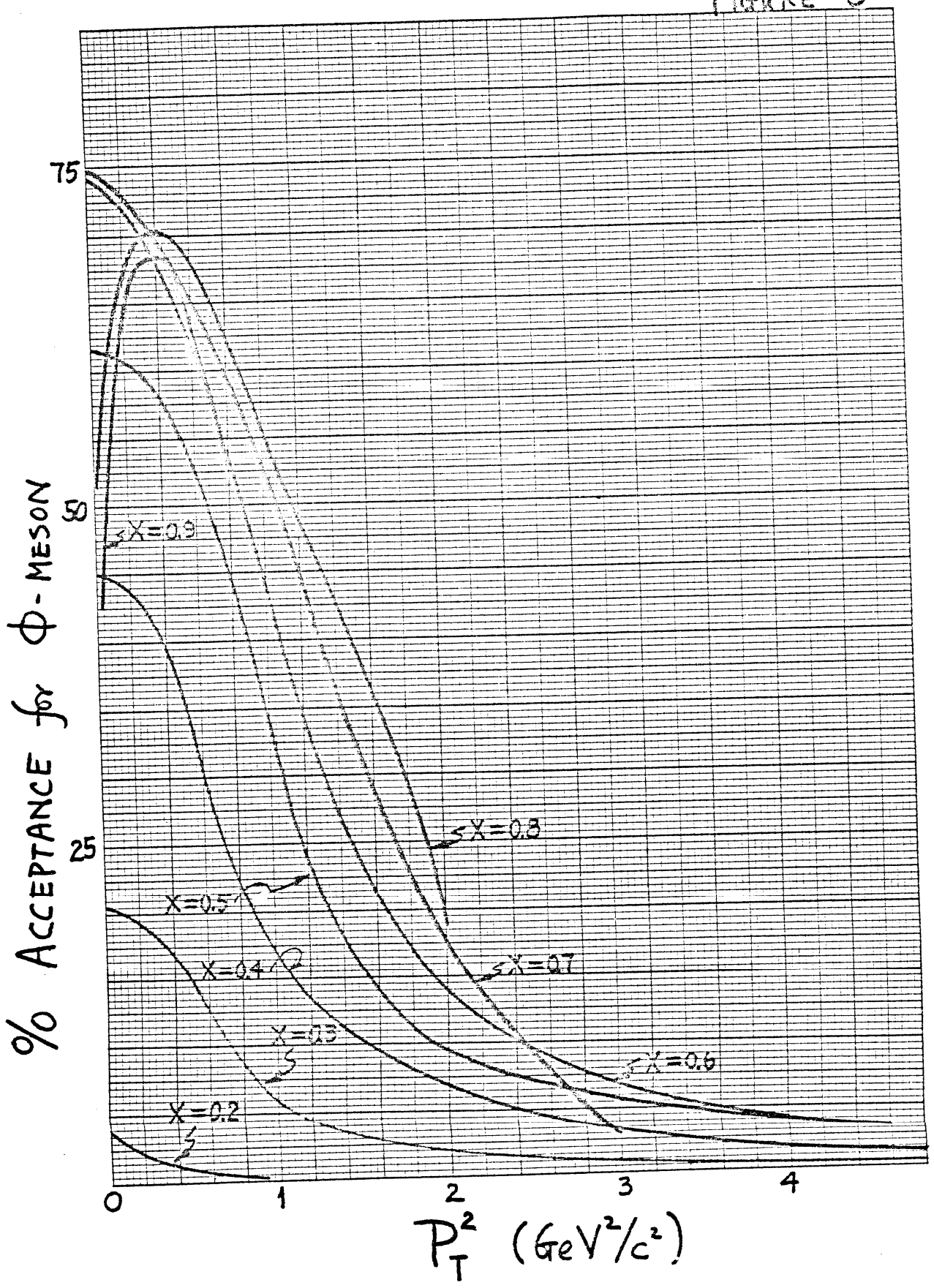
75
50
25
0
1
2
3
4
% ACCEPTANCE for Φ-MESON
P_T^2 (GeV²/c²)
X=0.9
X=0.8
X=0.7
X=0.6
X=0.5
X=0.4
X=0.3
X=0.2

APPENDIX I An Estimate of $\pi^+ p \to K^- + X$ Inclusive Cross Section

Since the trigger reaction in this proposal is

$$\pi^+ p \to K^- + X \qquad \text{(A.I.1)}$$

it is important to have as accurate as possible an estimate on its inclusive cross section. Although reaction (A.I.1) is in principle not difficult to measure, to date no published data exist in either SLAC/BNL or FNAL energy regions. Recently, a preprint from the CERN-OMEGA Spectrometer group[1] makes possible a crude measurement of the inclusive cross section for the reaction

$$\pi^- p \to K^- + X \qquad \text{(A.I.2)}$$

at 19 GeV/c. In that experiment, a total of 3.2×10^6 triggers were recorded, 40% of which was target originated. The cross section sensitivity of the experiment is reported to be 28 events/nb and the "average" K^- acceptance is 3.6%. One, therefore, has

$$\sigma_{K^-} = 3.2 \times 10^6 \times 40\%/(3.6\% \times 28 \times 10^{+6}) = 1.27 \text{ mb} \qquad \text{(A.I.3)}$$

The actual value must await a careful acceptance correction and is not available at this point. The question here is: <u>given the inclusive K^- cross section from π^-, what can we say about that from a π^+ beam?</u>

A priori, one would expect that K^- triggers would be more copious from $\pi^- p$ interaction. Although triggering on a K^- eliminates that portion of the strange particle production commonly referred to as associated production, e.g. $\pi^+ p \to K^+ \Sigma^+$ and $\pi^- p \to K^+ \Sigma^-$, $\pi^- p$ interaction differs from $\pi^+ p$ in that $A_2^- \to K^- K^\circ$ can be produced diffractively via ρ-exchange. The corresponding process in $\pi^+ p$ interaction is the A_2^+ production. Since A_2^+ does not have a decay mode involving a K^- meson, its production cannot contribute to the trigger rate in our proposal except due to inefficiencies of the Cerenkov counter in rejecting pions. In fact,

the realization of the A_2^- production in π^-p interaction is one of the reasons that persuaded us to use a π^+ beam instead.

Table A.I.1a lists up to six-body final states from π^-p and π^+p interactions with a pair of K^+K^- mesons. Reactions with a K^-K° pair are listed in Table A.I.1b. No data exist on conjoint productions, i.e., final states with two strange particles and a ϕ meson, these reactions will not be considered here. We shall argue later in this Appendix that inclusion of the conjoint production will not alter our conclusions.

It is obvious from Table A.I.1 that there are many more channels available to π^-p interaction for producing either a K^+K^- or a K^-K° pair. For three-body final states, π^-p can proceed via two different channels, one for each of K^+K^- and K^-K° states, while no corresponding channels with a K^- exists for π^+p interaction. In the four-body category, π^+p has one available channel versus four for π^-p interaction.

To examine the relative magnitude of these reactions, we plot all available data[2] on Figure A.I.1. The circle and square symbols are for K^+K^- production while the triangles are for K^-K° states. As may be noticed, there exists virtually no data above 10 GeV/c for either π^-p or π^+p interactions. After careful examination of these cross sections, some systematic trends emerge:

1. For a given number of pions produced, cross sections for different charge combinations are the same separately for the reactions

$$\pi^\pm p \to K^+K^- + X \qquad \text{(A.I.4)}$$

and

$$\pi^\pm p \to K^-K^\circ + X. \qquad \text{(A.I.5)}$$

This trend may be seen in Figures A.I.1b and A.I.1c where data exist for both π^-p as well as π^+p reactions.

2. At least in the energy region below 10 GeV/c, cross sections for producing a K^+K^- pair is consistently higher than those for a K^-K° pair in each topology. This is understandable in view of the fact that the first prominent resonance state in K^+K^- state (S^*-meson) is less massive than that in the K^-K° state (A_2 meson), therefore, requires less C.M. energy for a threshold rise. Since no systematic studies exist for these reactions with high statistics, we can not confirm this conjecture experimentally.

3. For $K\bar{K}N$ and $K\bar{K}N\pi$ states where more cross section information is available, one observes, in each case, the cross sections exhibit a threshold rise, reach a maximum followed by a decline with higher energies. In the case of $K\bar{K}N$ reactions, the cross section maximum appears at lower incident momentum than that for the $K\bar{K}N\pi$ states. This is expected based on phase space arguments. One may deduce that in each topology, the inclusive cross section ratios for π^+p and π^-p producing a K^+K^- and K^-K° pairs are separately given by the ratio of the number of available channels. For example, for K^+K^-N mode, π^-p inclusive cross section may be twice that for π^+p. If one further assumes that cross sections for each topology follow the same rise-peak-fall off pattern seen in $K\bar{K}N$ and $K\bar{K}N\pi$ states, and that higher multiplicity states reach maxima at higher incident momenta, it is then reasonable to assume that the $K\bar{K}N$, $K\bar{K}N\pi$, $K\bar{K}N2\pi$ and $K\bar{K}N3\pi$ states have roughly the same cross sections at 15 GeV/c. Therefore, the cross section ratios are given by the ratios of available channels, or

$$\sigma(\pi^-p \to K^+K^- + X)/\sigma(\pi^+p \to K^+K^- + X) = 10/6 \qquad \text{(A.I.6)}$$

and

$$\sigma(\pi^-p \to K^-K^\circ + X)/\sigma(\pi^+p \to K^-K^\circ + X) = 10/3 \qquad \text{(A.I.7)}$$

Since one does not know whether K^-K° cross sections are higher than those of K^+K^-, it can be estimated that $\pi^-p \to K^- + X$ trigger rate may be between 3.3 and 1.6 times that of $\pi^+p \to K^- + X$. Taking $\pi^-p \to K^- + X$ inclusive cross section to be 1.27 mb, one anticipates

$$0.38 \text{ mb} < \sigma(\pi^+p \to K^- + X) < 0.76 \text{ mb} \qquad \text{(A.I.8)}$$

Turning to the conjoint production, there exists some evidence[3,4] that cross sections for producing a pair of strange particle in association with a ϕ-meson may be as high as that for producing a ϕ-meson alone. This massive cluster, treated as a single entity may be produced diffractively from either a π^+ or a π^- beam. It may also be produced in the central region. Since cross sections for producing a K^+K^- pair are approximately the same for π^+p and π^-p interaction, the inclusion of conjoint production is equivalent to a proportional increase in K^+K^- production cross sections. Therefore, the estimate made for reaction A.I.1 remains unchanged.

REFERENCES

1. B. Ghidini et al., CERN/EP/PHYS 76-12 (1976).
2. D. M. Chew et al., LBL-53 (1973). E. Bracci et al., CERN/HERA 72-1 (1972). R. Diamond et al., Phys. Rev. D 7, 1977 (1973).
3. R. Donald et al., Phys. Letters 61B, 210 (1976).
4. OMEGA Spectrometer group, CERN. In this experiment, 120 ϕ events are found in $\pi^- p$ interaction at 19 GeV/c. These authors reported a cross section ratio of $\sigma(\pi^- p \to \phi\pi^+\pi^-\pi^- p)/\sigma(\pi^- p \to \phi K^+ K^- \pi^- p) = 1.4 \pm 0.3$.

Table A.I.1a. A List of Reactions with a K^-K^+ Pair in the Final State

	π^-p Induced	π^+p Induced
Three-Body	K^+K^-n	
Four-Body	*$K^+K^-n\pi^\circ$	$K^+K^-p\pi^+$
	$K^+K^-p\pi^-$	
Five-Body	*$K^+K^-n\pi^\circ\pi^\circ$	$K^+K^-n\pi^+\pi^+$
	$K^+K^-n\pi^+\pi^-$	$K^+K^-p\pi^+\pi^\circ$
	$K^+K^-p\pi^-\pi^\circ$	
Six-Body	*$K^+K^-n\pi^\circ\pi^\circ\pi^\circ$	§$K^+K^-p\pi^+\pi^-\pi^-$
	*$K^+K^-n\pi^\circ\pi^+\pi^-$	$K^+K^-p\pi^+\pi^\circ\pi^\circ$
	$K^+K^-p\pi^-\pi^+\pi^-$	*$K^+K^-n\pi^+\pi^+\pi^\circ$
	*$K^+K^-p\pi^-\pi^\circ\pi^\circ$	

*Multi-neutral final state, no data exist

§No data

Table A.I.1b. A List of Reactions with a K^-K° Pair in the Final State

	π^-p Induced	π^+p Induced
Three-Body	$K^-K^\circ p$	
Four-Body	$K^-K^\circ\pi^+n$	
	$K^-K^\circ p\pi^\circ$	
Five-Body	$*K^-K^\circ\pi^+n\pi^\circ$	$K^-K^\circ p\pi^+\pi^+$
	$K^-K^\circ\pi^+p\pi^-$	
	$*K^-K^\circ p\pi^\circ\pi^\circ$	
Six-Body	$*K^-K^\circ n\pi^+\pi^\circ\pi^\circ$	$K^-K^\circ p\pi^\circ\pi^+\pi^+$
	$*K^-K^\circ p\pi^\circ\pi^\circ\pi^\circ$	$K^-K^\circ n\pi^+\pi^+\pi^+$
	$K^-K^\circ n\pi^+\pi^+\pi^-$	
	$K^-K^\circ p\pi^\circ\pi^+\pi^-$	

---

*Multi-neutral final state, no data exist.

§No data.

FIGURE A.I.1

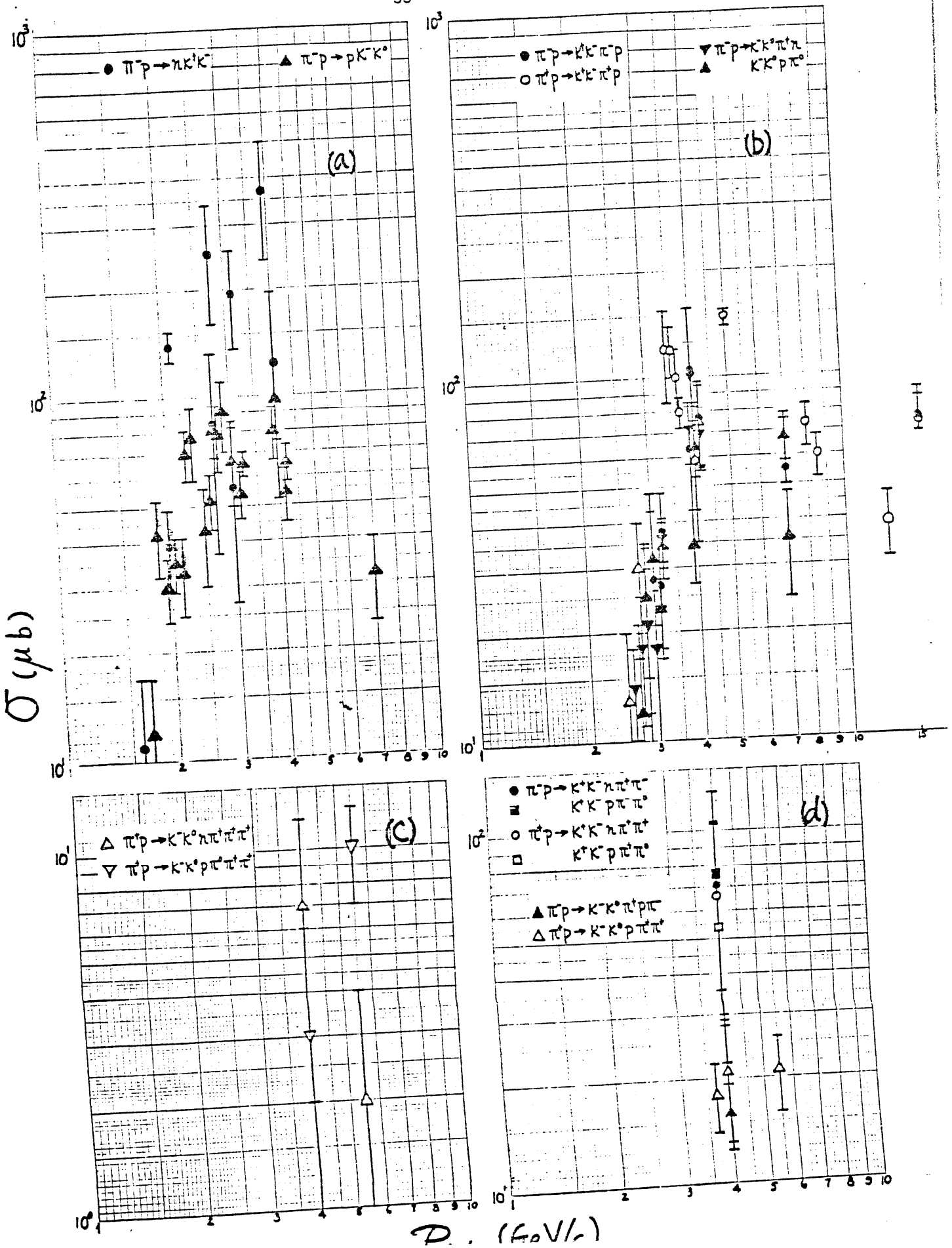

APPENDIX II AN ESTIMATE OF $\pi^+ p \to \phi + X$ INCLUSIVE CROSS SECTION

The aim of this appendix is to arrive at the best estimate for the inclusive cross section for the reaction

$$\pi^+ p \to \phi + X \qquad \text{(A.II.1)}$$

at 15 GeV/c. At this time, no direct, published results exists. The following list of experiments represents nearly all available and relevant data:

1. At 24 GeV/c, Blobel et. al[1] reported that the inclusive cross section for the reaction

$$pp \to \phi + X \qquad \text{(A.II.2)}$$

is 158 ± 35 μb.

2. At 150 GeV/c, Anderson et. al[2] studied Reaction (A.II.2) and the reaction

$$\pi^+ p \to \phi + X \quad |\to \mu^+\mu^- \qquad \text{(A.II.3)}$$

using the Chicago Cyclotron Spectrometer. The differential Cross Sections for reactions A.II.3 and A.II.2 are parameterized respectively by

$$E\frac{d\sigma}{d^3p}\Big|_{\pi^+ p} \sim (1-x)^{1.73 \pm .44} \; e^{-(3.61 \pm .40)P_T} \qquad \text{(A.II.4)}$$

and

$$E\frac{d\sigma}{d^3p}\Big|_{pp} \sim (1-x)^{4.06 \pm .40} \; e^{-(3.93 \pm .28)P_T} \qquad \text{(A.II.5)}$$

The inclusive ϕ cross sections for $x > 0$ are given as 330 ± 100 μb and 280 ± 80 μb for pp and $\pi^+ p$ reactions respectively.

3. Preliminary results[3] from CERN Omega Spectrometer are used. The reaction studied is

$$\pi^- p \rightarrow \phi + X \qquad \text{(A.II.6)}$$

at 16 GeV/c. The data are obtained using a K^- trigger. A total of ~2200 events are observed above the background. Corrected for acceptance losses, the P_T dependency is given by

$$\frac{d\sigma}{dP_T^2} \sim e^{-(2.4 \pm 0.3)P_T^2} \qquad \text{(A.II.7)}$$

for $x > 0.5$ where the acceptance corrections are reasonably small and well understood. The mass and the x distributions corrected for geometric acceptance are shown in Figure A.II.1 a and b respectively. Corrected for low P_T losses, the resultant x distribution is shown as solid dots in Figure A.II.1b.

4. In a high statistics bubble chamber experiment, C. Baltay[4] has collected and measured ~600,000 events produced in $\pi^+ p$ interaction at 15 GeV/c. Since K_L^o detection efficiency in a bubble chamber is typically a few percent, the only viable method of detecting ϕ-meson inclusive production is by examining the mass spectrum of a pair of oppositely charged particles interpreted as charged kaons. Such information is not yet available from this experiment.

To estimate the inclusive ϕ cross section in $\pi^+ p$ interaction at 15 GeV/c, we make use of the FNAL $\pi^+ p$ data at 150 GeV/c and the CERN $\pi^- p$ data at 16 GeV/c. Figures A.II.2 a and b show the differential cross sections in x and P_T^2 for the FNAL data. The smooth curves represent phenomenological fits to the expressions

$$E \frac{d\sigma}{dx dp_T^2} \sim e^{-(3.4 \pm .7)x - (2.3 \pm .3)P_T^2} \qquad \text{(A.II.8)}$$

as may be seen, with the exception of the lowest P_T^2 point, the data are well described by Equation A.II.8. We note that the P_T^2 slope in 16 GeV/c $\pi^- p$ data is $2.4 \pm .3\ (\text{GeV/c})^{-2}$ and is consistent with a value of $2.3 \pm .3\ (\text{GeV/c})^{-2}$ from the 150 GeV/c $\pi^+ p$ data. To compare the x dependency, Monte Carlo technique is used. We note that Equation A.II.8 integrated over P_T^2 is equivalent to the expression

$$\frac{d\sigma}{dx} \sim e^{-4.9\,x} \qquad \text{(A.II.9)}$$

The solid line in Figure A.II.1b represents a fit to this expression for $x > 0.365$. The two lowest x points are not used due to the very large correction factors needed (a factor of 20 at $x = 0.192$ and 5 at $x = 0.308$). Therefore, we conclude that at least for $x > 0.365$, the $\pi^- p$ data at 16 GeV/c can also be well described by Equation A.II.8 . Extrapolating to $x = 0$, we obtain

$$\sigma_{\pi^- p \to \phi + X} = \begin{cases} 90 \pm 13\ \mu b & \text{for } x > 0 \\ 33 \pm 5\ \mu b & x > 0.2 \\ 6.8 \pm 1.5\ \mu b & x > 0.5 \end{cases}$$

These may be compared with $79 \pm 18\ \mu b$ for $x > 0$ in pp interaction at 24 GeV/c.

REFERENCES

1. V. Blobel et.al., Phys. Letters 59B, 88(1975).

2. K. J. Anderson et.al., Phys. Rev. Letters 37, 799(1976).

3. P. Woodworth, CERN Omega Spectrometer Group, private communication.

   D. Miller, Purdue University, private communication.

4. C. Baltay, Columbia University, private communications.

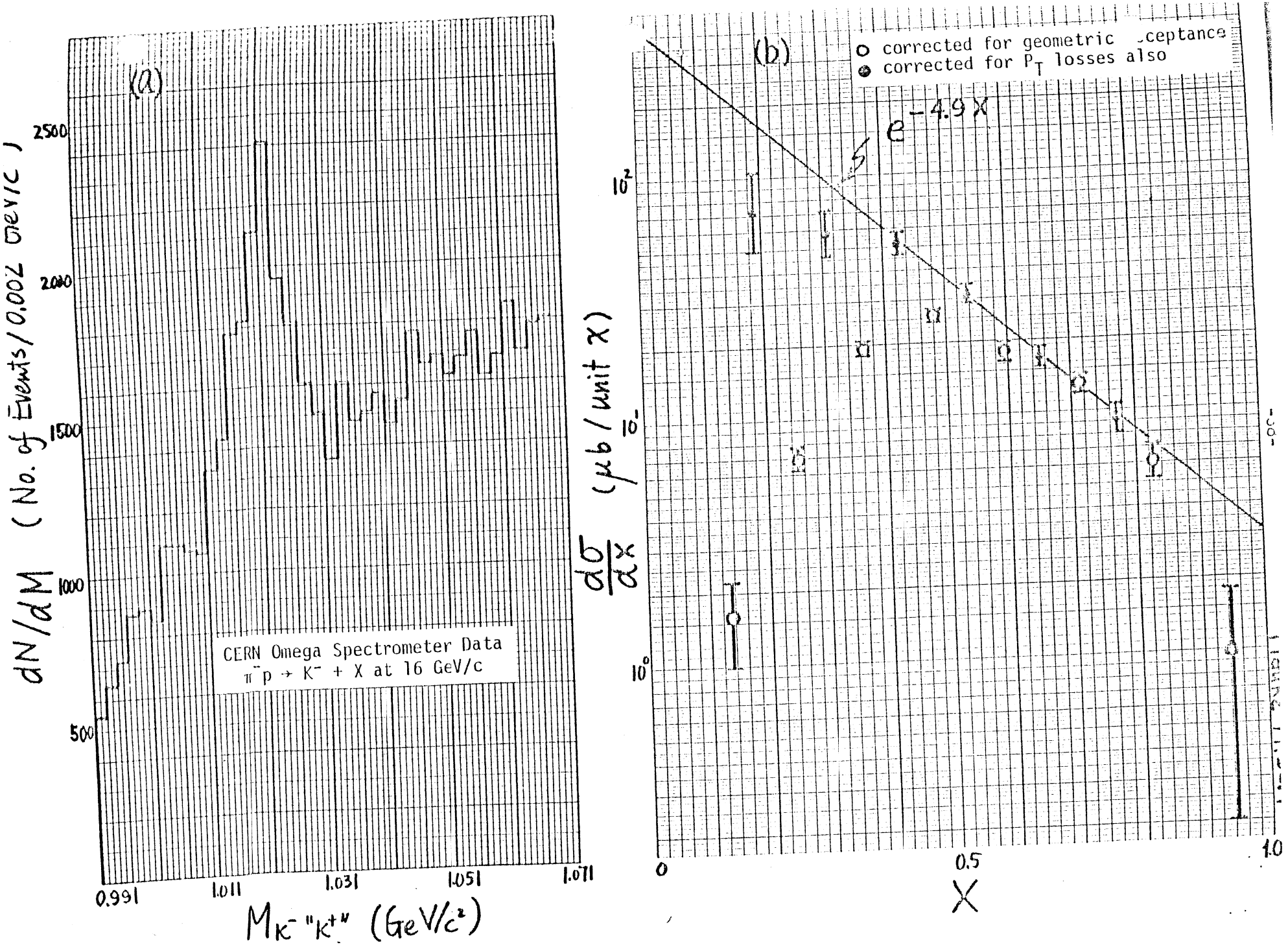
(a)
dN/dM (No. of Events/0.002 GeV/c²)
2500
2000
1500
1000
500
CERN Omega Spectrometer Data
π⁻p → K⁻ + X at 16 GeV/c
0.991
1.011
1.031
1.051
1.071
M K⁻ "K⁺" (GeV/c²)
(b)
corrected for geometric acceptance
corrected for P_T losses also
e^-4.9X
dσ/dx (μb / unit x)
10²
10¹
10⁰
0
0.5
1.0
X

FIGURE A.11.7

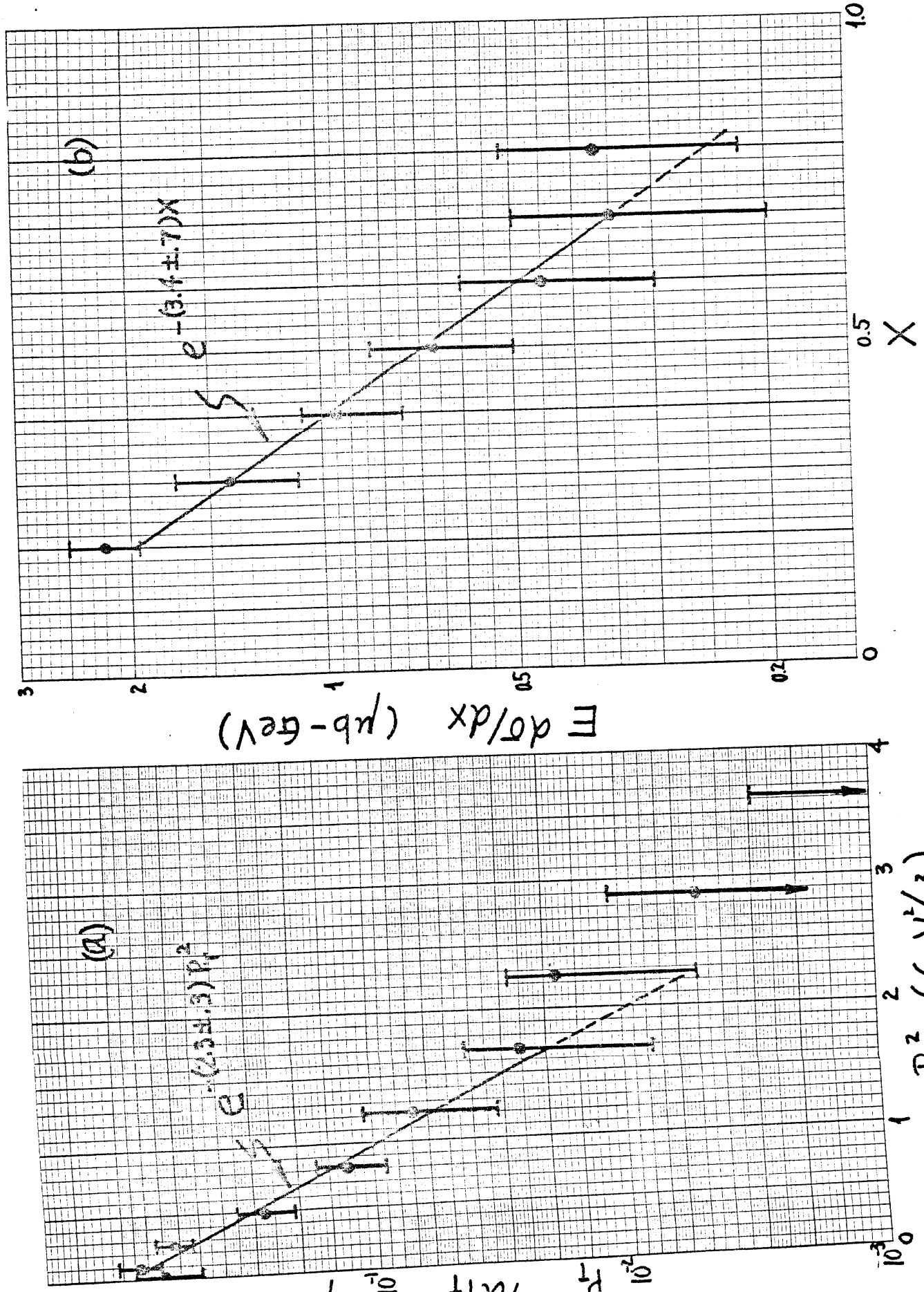
(b)
$e^{-(3.1 \pm .1)x}$
$E\, d\sigma/dx$ (μb-GeV)
X
1.0
0.5
0
3
2
1
.5
.2
(a)
$e^{-(2.5 \pm .3) p_T^2}$
$\frac{1}{P_T} d\nu/dP_T$ (μb/GeV/c)
P_T^2 (GeV²/c²)
10^{-1}
10^{-2}
10^{-3}
0
1
2
3
4

APPENDIX III. AN ISOBUTANE CERENKOV COUNTER FOR PION VETOES

1. Basic Considerations

The trigger logic $\pi^+ \cdot \sum_i V_{1i} \cdot V_{2i} \cdot V_{3i} \cdot V_{4i}$ effectively defines a negatively charged particle. The momentum distributions for the K^- and π^- accepted by this logic are given by Figures A.III.1 a and b respectively. The π^- sample is generated using experimental data whereas K^- curve assumes an isotropic production of a K^+K^- system in the c.m.. Corrections for decays in flight have been applied to the K^- spectrum only. The π^- inclusive cross section is 24.50 ± .34 mb, and the K^- inclusive cross section is estimated in Appendix I to be 0.57 ± 0.19 mb. Folding in the acceptance (13.7% for π^- and 4.45 % for K^-), one expects a π^- to K^- ratio of 132 to 1. Therefore, it is of overriding importance that the Cerenkov counter considered here can effectively veto virtually all of the π^- accepted by the picket fence counter logic. Since the ratio of the threshold momenta for π^- and K^- is equal to the inverse of the mass ratio, it is not possible to save all K^- triggers and at the same time veto all π^- particles. Practical factors that have important bearings on the design considerations include:

A. A high K^- acceptance. A larger solid angle acceptance can be achieved by either placing the counter closer to the streamer chamber or building a larger counter. The close proximity to the streamer chamber magnet coils and the fact that the magnet return yokes are normally saturated place a severe constraint on the physical location of the counter. The proposed layout of the apparatus is consistent with the requirement for an environment of weak magnet field ($\leq$ 50 gauss). The size of the entrance window is determined by a study of the K^- hit density from ϕ decays.

B. A good π^- rejection efficiency. Since the signature for a K^-(or $\bar{P}$) in this counter is a null signal, a high π^- detection efficiency is essential.

Taking into consideration the expected π^- to K^- ratio of 132, a π^- efficiency of 99.9% is chosen. This will result in a 12% contamination in the K^- trigger. The major contributing factors to the inefficiencies of a Čerenkov counter are (a) insufficient number of photoelectrons from a π^- resulting from a combination of insufficient radiator length and transmission/collection losses, and (b) interaction at the window or other material in front of the counter resulting in secondary particles which deviated from the designate photo tube or are below threshold for Čerenkov radiation. To overcome some of these problems, an atmospheric pressure isobutane counter of 2 m radiator length is chosen. The window for an atmospheric counter can be made of as thin as a few mils of aluminum. In the case of a high pressure Čerenkov counter, a strong and thick window is usually required for structural strength. As will be substantiated later in this Appendix, a π^- efficiency of 99.9% can be achieved with our design and such expectations can be justified using existing Čerenkov counters of a similar type.

C. A low K^- veto loss. A legitimate K^- signal can be lost due to scintillation in the gas or δ-ray production at the window or other material immediately in front of the counter. Isobutane is chosen because of its low scintillation efficiency. As will be substantiated later in this appendix, δ-ray production is not expected to cause a significant loss of K^- trigger. The atmospheric pressure requires only a thin window for the counter, thereby, minimizing the δ-ray production.

2. Design Considerations.

The standard formula for Čerenkov counter[1,2] are

$$\text{Cos } \theta = \frac{1}{\beta n} \qquad \text{(A.III.1)}$$

and

$$N = 2\pi\alpha \ \ell \ \text{Sin}^2 \theta \int E(\lambda) f(\lambda, p) \frac{d\lambda}{\lambda^2} \qquad \text{(A.III.2)}$$

where N is the number of photoelectrons, β and θ are the velocity and the Čerenkov angle of the charged particle, n and ℓ are the index of refraction and the path length of the particle in the gas. The quantity $E(\lambda)$ is the quantum efficiency of the photomultiplier tube. The function $f(\lambda,p)$ is the transmittance for Čerenkov light of wavelength λ in a gas of pressure p. Its dependency on the pressure is given by[3]

$$f(\lambda,p) = f(\lambda,p = 1 \text{ atm.})^{\rho_p/\rho_1} \qquad \text{(A.III.3)}$$

where ρ_p and ρ_1 are the density of the gas at a pressure p and 1 atmosphere respectively. The index of refraction of the gas as a function of the pressure is given by E. R. Hayes et. al.[4]

In the design of the counter, we are guided by the reported operating characteristics of two similar atmospheric Čerenkov counters: (a) an isobutane counter of SLAC-Group A[5] and (b) a CERN butane counter[6] used by Winter's group in a series of $K^0_{S,L}$ decay studies. The reported efficiencies for trigger particles ---electrons in both instances, are "better than 99%" for the CERN counter and 99.6 ± 0.4% averaged over the entrance window for the SLAC Group A counter. Since in both instances, the Čerenkov counters were used to indicate the presence of a trigger particle, it was not as important to overcome that last one percent of inefficiency as it is in our case. We have attempted to understand the sources of these inefficiencies.

A. Photoelectron Statistics. Figure A.III.2 shows the number of photoelectrons calculated using Equation A.III.2 with the appropriate phototubes used in these counters. One notes that,

(a) If single photoelectron can be detected, the inefficiency of a counter is given by

$$\text{Inefficiency} = e^{-\varepsilon N} \qquad \text{(A.III.4)}$$

where ε is the light collection efficiency of the counter and N is the expected number of photoelectrons. Using the calculated collection efficiency of 16% as was quoted for the CERN counter, the expected efficiency should be 99.96%.

(b) The inefficiency can be caused by the discriminator threshold settings. This has been noted in reference 5 by D.Trines. Below the saturation point, the phototube output pulse height is proportional to the number of photoelectrons produced by the photocathode. Therefore, setting a discriminator threshold for an affirmative Čerenkov signal is equivalent to requiring a minimum number of photoelectrons, N_o. For example, the expected efficiency for the CERN counter drops to 99% if a threshold requirement corresponding to $N > 2$ is set. Assuming Poisson statistics, the pulse height distribution given in reference 5 for the SLAC counter (peak at 2.16 volts with a width of 0.76 volt FWHM for 15 GeV/c π^+) corresponds to 38 detected photoelectrons. With 63 available photoelectrons as is shown in Figure A.III.2, this corresponds to an average collection/transmission efficiency of 60%. Trines noted that inefficiencies can be improved upon by lowering the discriminator threshold setting. For the point with the lowest efficiency (98.13 ± .27% at 800 mV setting), they were able to improve the efficiency to 99.9 ± .03% by reducing the discriminator threshold setting to 100 mV. It should be noted that the inefficiency at 800 mV is too great to be consistent with having 38 detected photoelectrons at 2.16 Volts. Therefore, at a level of 10^{-3}, the photoelectron statistics is not the principle source of inefficiencies for the SLAC counter.

B. Nuclear Scattering.

In the case of the SLAC counter, the incident beam particles (15 GeV/c π^+) are defined by two 2" x 6" x 1/8" scintillation counters separated by 68". Inefficiencies can result if a pion scatters at the front scintillation counter, and the resultant products hit the hodoscope behind the Čerenkov counter but are below threshold for a Čerenkov signal. For isobutane operated at one atmosphere, the pion threshold is 2.55 GeV/c. The π^+ interaction probability in a 1/8" thick scintillator is 0.47%. Using the $\pi^\pm$ inclusive distributions for 15 GeV/c π^+ p data[7] and the actual experimental layout,[5] the probability for at least one of the produced $\pi^\pm$ to hit the downstream 2" x 6" counter is 34.5%, and 0.89% gives no Čerenkov light. Adjusting for the averaged $\pi^\pm$ multiplicity of 3.57, the contribution by this mechanism to the inefficiency of the SLAC Čerenkov counter is estimated to be

$$0.47\% \times 0.89\% \times (1-34.5\% \times 2.57/3.57) = 3.14 \times 10^{-5}$$

We therefore conclude that at a level of 10^{-3} inefficiency, there is no single dominant factor. The uncertainty (±0.03%) may be due to systematic limitations such as K^+ or p contaminations in the beam.

C. Light Collection System

It is apparent from Equation A.III.2 that the number of photoelectrons decreases rapidly with increasing wavelength. Therefore, the light collection system should be designed to accept as low a wavelength as one practically can. The 50% transmission point for 1 m of isobutane gas is at 1820 Å. To be able to collect light down to the ultra-violet region, it was noted in a published study by E. Garwin et. al[8] that the use of a less expensive phototube 56 AVP coated with a wavelength-shifter paraterphenyl (pTP) can deliver ∿95% of the pulse height expected from a more expensive phototube, such as 56 DUVP with a quartz window.

3. Physical Structure and Dimensions of the Proposed Čerenkov Counter

The main frame of the counter is constructed with aluminum angles and measures 1.25 m high by 2 m wide by 2 m long. The entrance and exit windows are made of 2 mil aluminum. The counter is covered at the exit by 10 spherical mirrors in a 2 x 5 matrix. The Čerenkov light reflected by the mirrors is collected by parabolic Winston funnels.[9] The end of each funnel is joined to a UVT disk coated with pTP. The phototubes (RCA 4522) and bases are mounted on the outside of the counter to avoid accidental sparks in the isobutane gas.

4. Expected Performance of the Čerenkov Counter

A. Light Collection/Transmission and Photoelectron Statistics.

The calculated number of photoelectrons is shown in Figure A.III.3a. As has been mentioned earlier, a careful study of available data on the SLAC 1 m isobutane Čerenkov counter reveals that inefficiencies are not due to obvious factors such as photoelectron statistics, nuclear scattering and light transmission/collection efficiencies. Systematic uncertainties such as K^+, p contamination in the beam may have been responsible for the sensitivity limit on the inefficiency measurement. We note that SLAC Group A experimenters were able to improve inefficiency at the worst point from $(1.87 \pm .27) \times 10^{-2}$ to $(1 \pm .3) \times 10^{-3}$ by lowering its discriminator threshold setting from 800 mV to 100 mV. This suggests that to reach a level of 10^{-3} inefficiency is entirely possible. It further suggests that the combination of many contributing factors may ultimately place a floor of 3×10^{-4} on the inefficiency. To estimate the expected performance of the counter, we used an 8% effective collection/transmission efficiency. In the case of the SLAC counter with 63 available photoelectrons and an averaged efficiency of 99.6 ± 4%, the corresponding value is 8.8%. Our design calls for a factor of two increase in the number of photoelectrons due to longer radiator and a 16% gain using RCA 4522 with pTP coating, it is reasonable to expect that these gains can adequately offset

any loss of actual collection/transmission efficiency, for a longer counter. The expected π^- veto inefficiency is shown in Figure A.III.3b. Our goal is to achieve 10^{-3} at the plateau region as is shown by the dotted line. Since K^- candidates are defined by the picket fence logic $V_{1i} \cdot V_{2i} \cdot V_{3i} \cdot V_{4i}$, the trigger tracks are well collimated. Therefore, we expect good light collection efficiency.

B. Nuclear Scattering

In the proposed layout, an element in V_{4i} (12.5 cm x 1.3 m and 2.5 m downstream of V_{3i} array) subtends a solid angle at V_{3i} equivalent to that due to the downstream hodoscope used with the SLAC counter. Since the momentum spectrum of pions in this experiment is between 2 and 9 GeV/c, the averaged charged particle multiplicity is lower than that at 15 GeV/c. We expect the effectiveness of the solid angle coverage for the produced particles from scattering by the V_{3i} picket fence counter elements is considerably reduced. Therefore the pion rejection inefficiency due to nuclear scattering is expected to be less than 10^{-4}.

C. δ - Ray Vetoes

As has been mentioned earlier in this Appendix that a good K^- track may be vetoed due to δ - rays produced at the window or the scintillation counters in front of the Čerenkov counter. The index of refraction of the atmospheric isobutane gas is 1.00148. Therefore, the threshold energy for a delta ray is 8.88 MeV. Using Bhabha's formula the probabilities for producing a δ - ray are shown in Figure A.III.4 for a 2 mil aluminum window and a ¼" thick scintillation counter placed immediately in front of the Čerenkov counter. This amount to a ½% effect and is primarily due to

scintillator.

D. Edge Effect on Light Collection

Due to the finite angle for Cerenkov radiation, pions hitting the edge of a given mirror may lose a significant fraction of the Čerenkov light to an adjacent mirror, thus resulting in inefficiency. For example, the expected spot size of the Čerenkov light at a mirror 2 m away varies from a radius of 5.6 cm for a pion momentum of 3 GeV/c to 10.7 cm for a 15 GeV/c pion. The intensity varies as 1/r within the spot. To minimize this effect, every fourth element of the V_{4i} array is to overlap two cells and is to be vetoed by a signal from either cell.

REFERENCE for APPENDIX III

1. H. Hinterberger et. al, Rev. of Sci. Inst. 41, 413 (1970).
2. M. Benot, J. Litt and R. Meunier, Nucl. Inst. and Methods 105, 431 (1972).
3. E.L. Garwin and A. Roder, Nucl. Inst. and Methods 93, 593 (1971).
4. E.R. Hayes, R.A. Schluter and A Tamosaitis, ANL-6916 (1964).
5. D. Trines, The Gas Cerenkov Counter for E-89 (1.6 GeV Spectrometer), SLAC Group A Note No. 11, March 1, 1973.
6. J.J. Aubert et. al, Nucl. Inst. and Methods 87, 79 (1970).
7. M. Kalelkar, Columbia University, private communications.
8. E.L. Garwin, Y. Tomkiewicz and D. Trines, Nucl. Inst. and Methods 107, 365 (1973).
9. H. Hinterberger and R. Winston, Rev. of Sci. Inst. 39, 419 (1968).
10. B. Rossi, High Energy Particles, Publisher: Prentice Hall, Inc. (1956).

FIGURE A.III.1

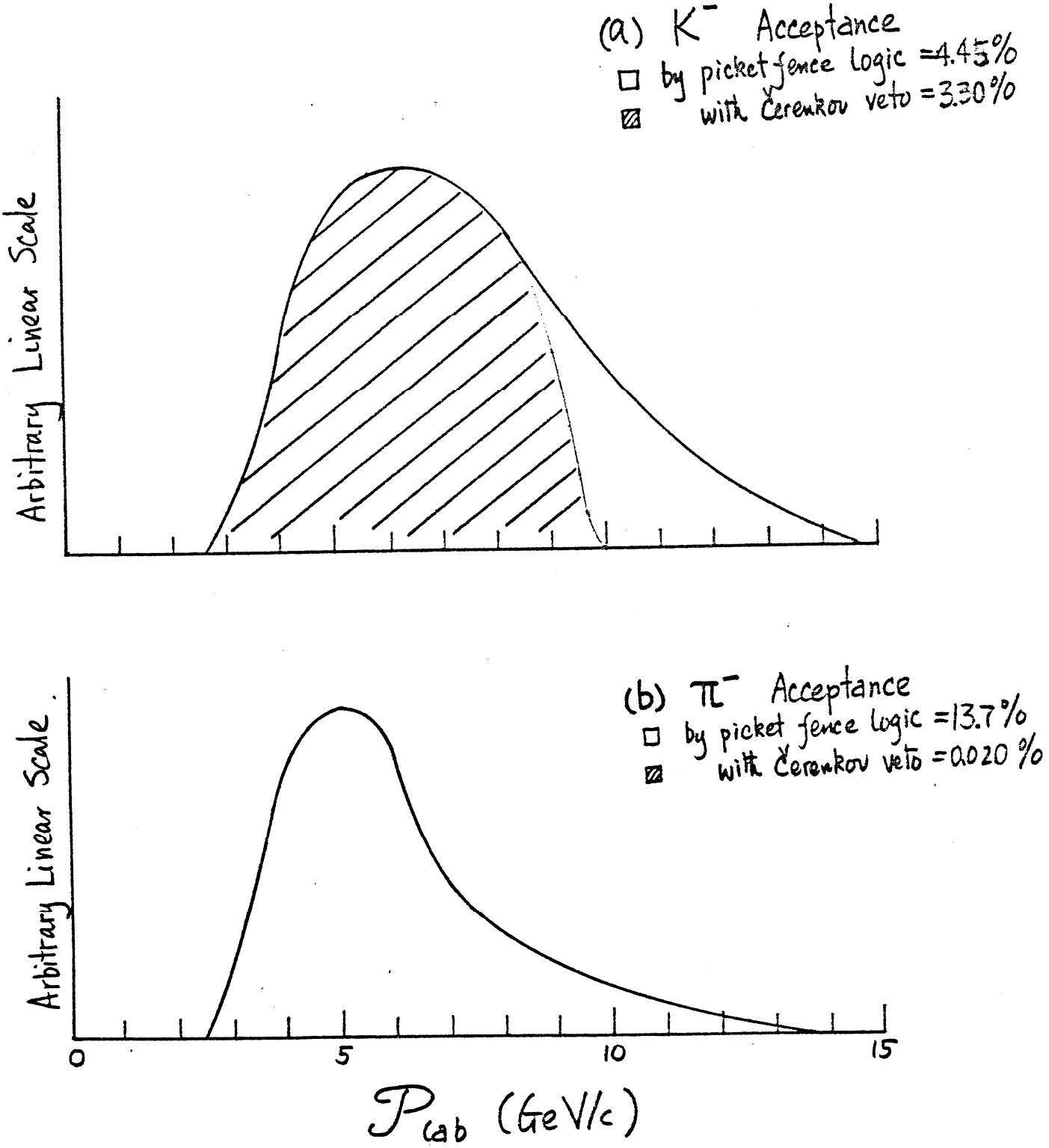

FIGURE A.III.2

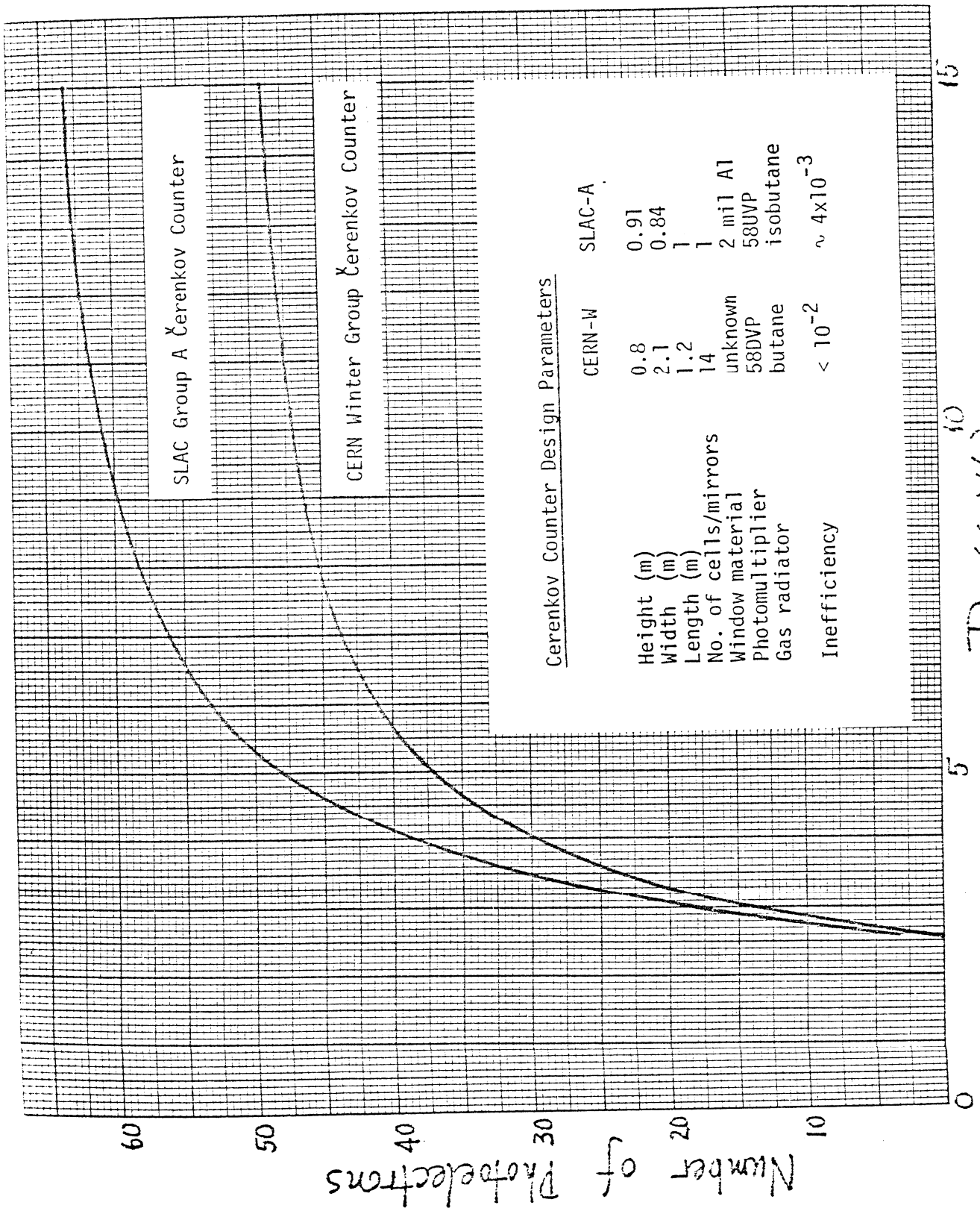

FIGURE A.III.1

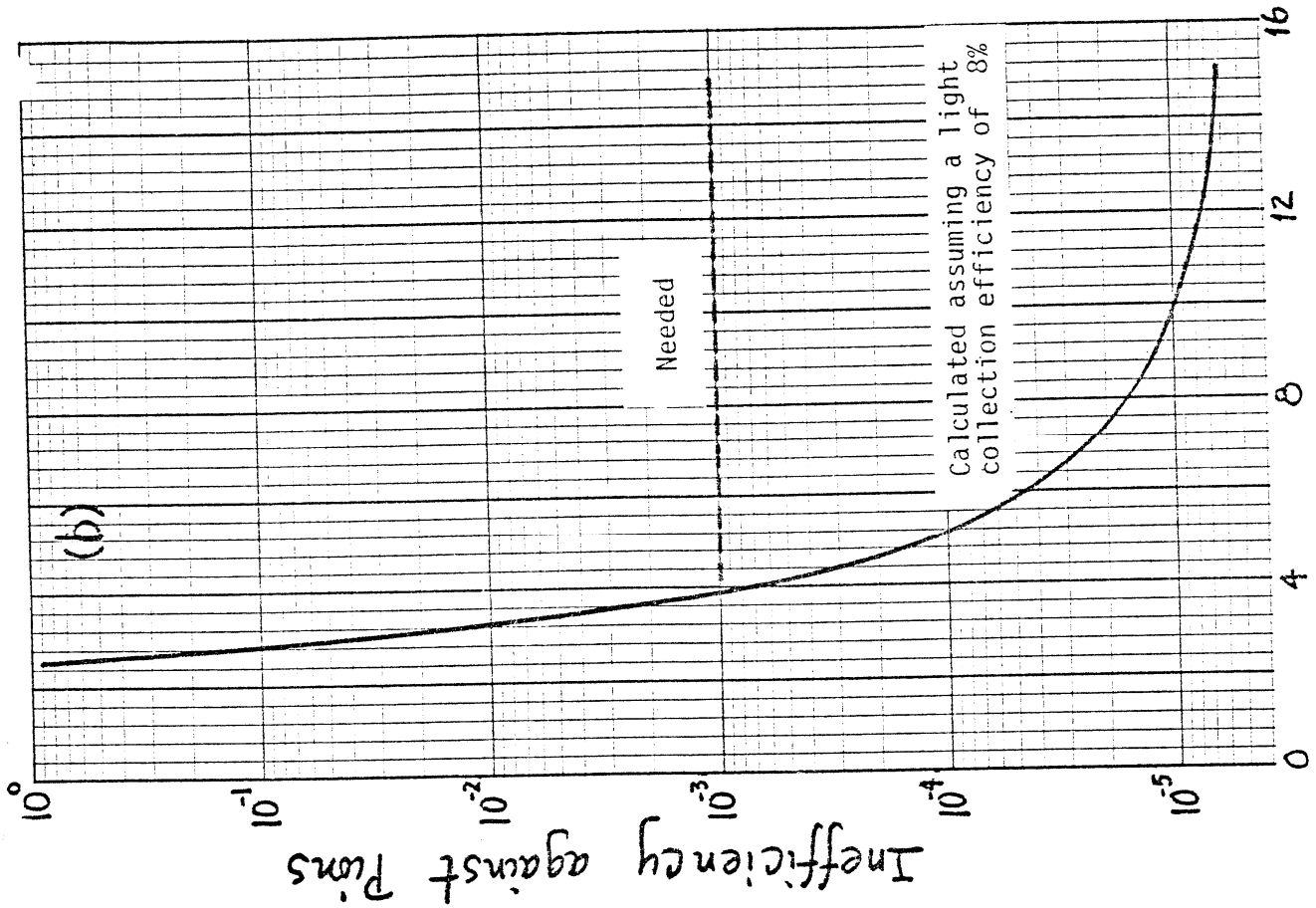

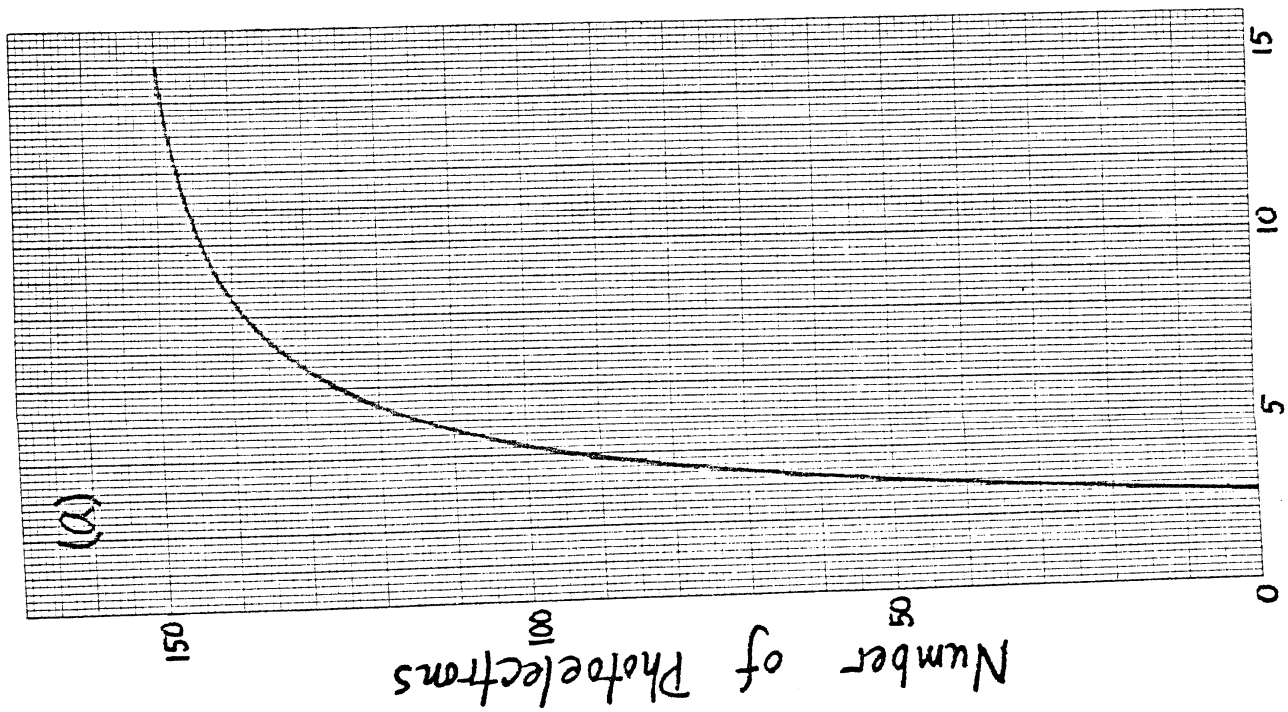

FIGURE A.III.4

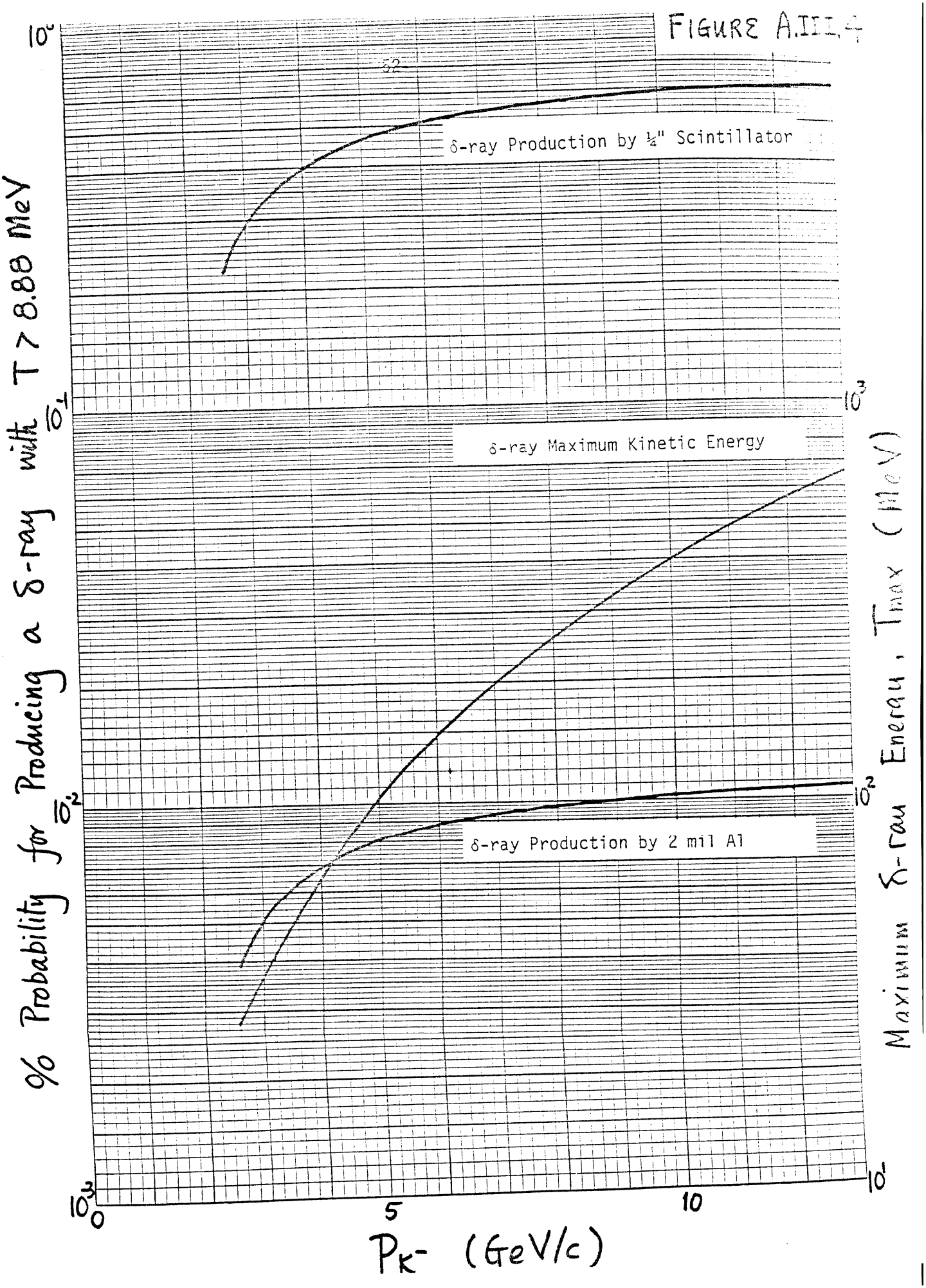

APPENDIX IV. CONSIDERATIONS OF SLAC 40" BUBBLE CHAMBER HYBRID FACILITY AS AN ALTERNATIVE DEVICE

In this Appendix, we attempt to assess the feasibility of doing this experiment using the SLAC 40" Bubble Chamber Hybrid Facility (SHF). This experiment requires a large aperture Čerenkov counter to identify the K^- particle and a large solid angle device for detecting accompanying charged particles. SHF meets both requirements, therefore, has been considered seriously as an alternative device.

The standard configuration for the SHF is shown in Figure A.IV.1. Three modules of multiwire proportional chambers are placed behind the bubble chamber. Using the fringe field of the bubble chamber magnet, the PWC's are capable of determining the momentum of a charged particle to 20% in 2 milliseconds. The high pressure Čerenkov counter (CANUTE) is capable of operating at 60 p.s.i.a. It has an entrance window of 1 m wide by 2.04 m high and is made of 5.7 mm thick aluminum. The counter has 10 mirrors each monitored by a separate phototube. In BC59 (π^+p at 11.6 GeV/c), the counter was filled with Freon 12 at 22 p.s.i.a. for identifying charged kaon triggers. Testing with tagged beam particles, R.A. Lewis concluded[1] that the counter is 98.4% efficient for 11.6 GeV/c π^+. Of the 1.6% inefficiencies, 1.5% is attributed to nuclear interactions at the entrance window resulting in no or too little Čerenkov light. The remaining 0.1% is due to too little light,not because of interactions. The dead time of the system due to camera advances is given as 3 second/frame.

In BC59, the system operates at 12 pulses/second with 7-8 π^+/pulse. A software cut is made to reject trigger kaons below 4.5 GeV/c to improve reliability in particle identification. For the 4c reactions

$$\pi^+ p \rightarrow \pi^+ p K^+ k^- \qquad \text{A.IV.1}$$

and

$$\pi^+ p \rightarrow \pi^+ p \pi^+ \pi^- \qquad \text{A.IV.2}$$

experimenters in BC 59 found[2] approximately equal numbers of events in the two reactions. The measured cross section ratio is 35:1 ($\sim$1.6 mb for reaction A.IV.2 and $\sim$45μb for eaction A.IV.1 at 11.6 GeV/c), therefore, this fact is consistent with the 98.4% efficiency quoted in reference 1.

To estimate the equivalent demand on the SHF for the ϕ study, we assume a fiducial volume of 60 cm, and a liquid hydrogen density of 0.07 gm/cc. At 8 π^+/pulse and 12 pulse/second, one can achieve a rate of 0.844 event/μb/hour. To estimate the acceptance, the phenomenological form obtained in 150 GeV/c study of the reaction[3]

$$\pi^+ p \rightarrow \phi + x \qquad \text{A.IV.3}$$

is used. The differential cross sections are parameterized by

$$E \frac{d^3\phi}{d \vec{p}} \sim (1-x)^{1.73 \pm .44} \; e^{-(3.61 \pm .40)P_T} \qquad \text{A.IV.4}$$

and is found to agree with preliminary results from the CERN Omega Spectrometer in the reaction

$$\pi^- p \rightarrow \phi + x \qquad \text{A.IV.5}$$

at 16 GeV/c. The resultant yields from the SHF and our proposed experiment are compared in Figure A.IV.1. For $x > 0$, the acceptance for ϕ-production using SHF is 7.42% as versus 8.85% for the streamer chamber facilities. The random veto of K^- by accidental π^+ or π^- has been corrected for our proposal. It amounts to a 6.4% reduction in the net acceptance. This effect has not been taken out of the SHF acceptance calculations. It is worth noting that to reach the central region, a system must be able to identify particles of low momentum. For the SHF, the limitation is due to nuclear scattering

at the entrance window, whereas in this proposal, we are constrained by the pion threshold in an isobutane Čerenkov counter. Our proposed experiment is capable of reaching lower x values (half maximum at x = 0.29) than that possible with the SHF (half maximum at x = 0.43). To obtain the same statistics (10.1K ϕ events and 50.3K total K^- sample, one would require

$$10.1 \times 10^3/0.844 \times 90 \times 1/2 \times 7.42\% = 3584 \text{ hours}$$

$$= 149 \text{ calendar days}$$

on the SHF. This does not include any systems down time. For momentum greater than 4.5 GeV/c, the anticipated π^- to K^- ratio is 24 to 1. The inefficiencies in the Čerenkov counter will add another

$$50.3 \times 10^3 \times 24 \times (1-98.4\%) = 1.93 \times 10^4 \text{ events}$$

due to pion contaminations. It is important to note that the reason for the Čerenkov counter inefficiency against pions in this case is the lack of sufficient Čerenkov light. Therefore this pion contamination is indistinguishable from the kaons and represents a permanent one that is not removable by off-line software cuts on the particle momentum versus the Čerenkov counter pulse height.

In summary, using operating parameters of the SLAC Hybrid Facility, our proposed experiment will take about 3600 hours at 12 pps, over 1/4 of the total sample is from Čerenkov counter inefficiencies and cannot be removed using software cuts. Furthermore the result will cover a narrower x range than the proposed experiment. We feel that it is difficult to justify occupying the SHF for so long while the same physics can be done more easily and requires 15% less lineac pulses with the streamer chamber facility.

REFERENCE FOR APPENDIX IV

1. R. A. Lewis, Particle Identification in Canute, SHF Memo #39, May 4, 1976.

2. D. Miller, private communication.

3. K. J. Anderson et. al, Phys, Rev. Letters 37, 799 (1976).

FIGURE A.IV.1

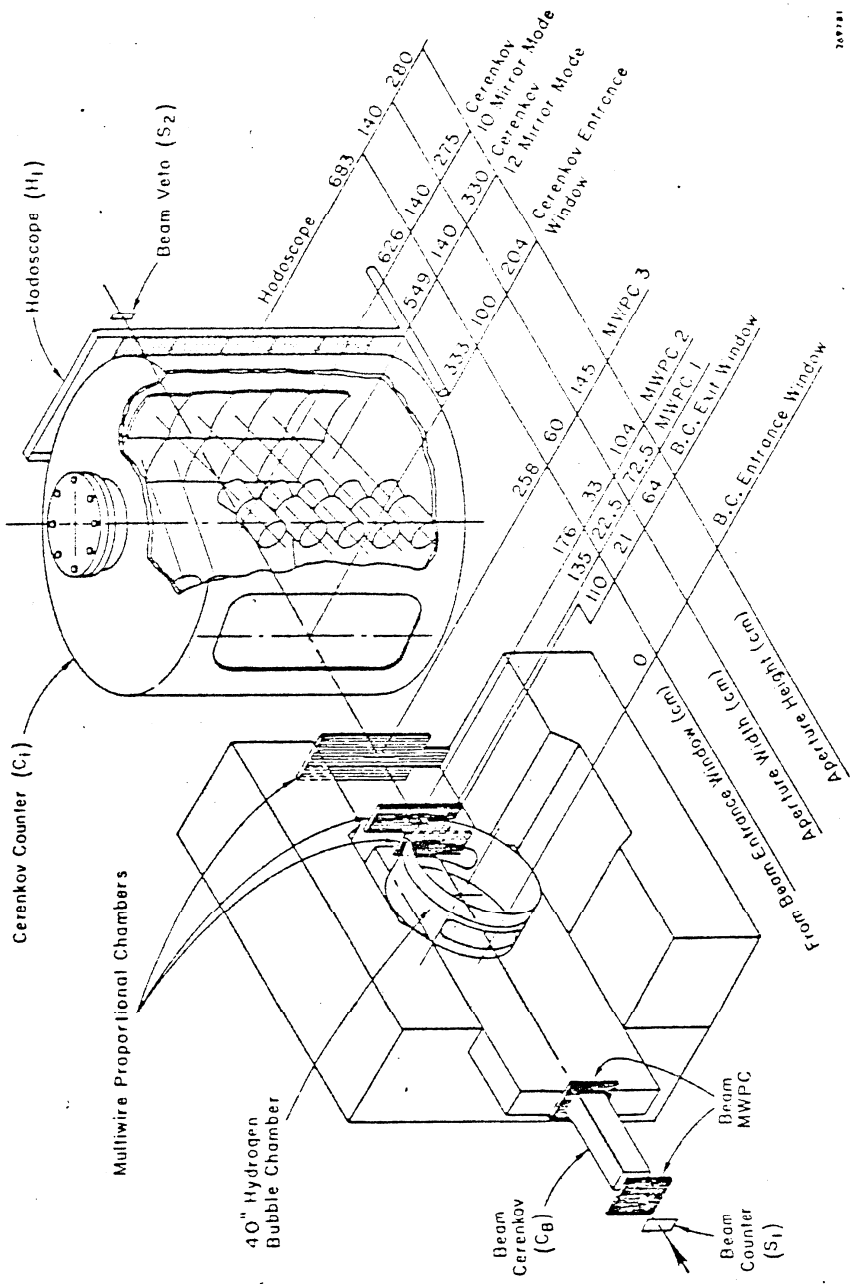
Hodoscope (H_1)
Beam Velo (S_2)
Cerenkov Counter (C_1)
Multiwire Proportional Chambers
40" Hydrogen Bubble Chamber
Beam Cerenkov (C_B)
Beam MWPC
Beam Counter (S_1)
Hodoscope
693
140
280
626
140
275
549
140
330
133
100
204
256
60
145
176
33
104
135
22.5
72.5
110
21
6.4
0
Cerenkov 10 Mirror Mode
Cerenkov 12 Mirror Mode
Cerenkov Window Entrance
MWPC 3
MWPC 2
MWPC 1
B.C. Exit Window
B.C. Entrance Window
Aperture Height (cm)
Aperture Width (cm)
From Beam Entrance Window (cm)

FIGURE A.IV.2.

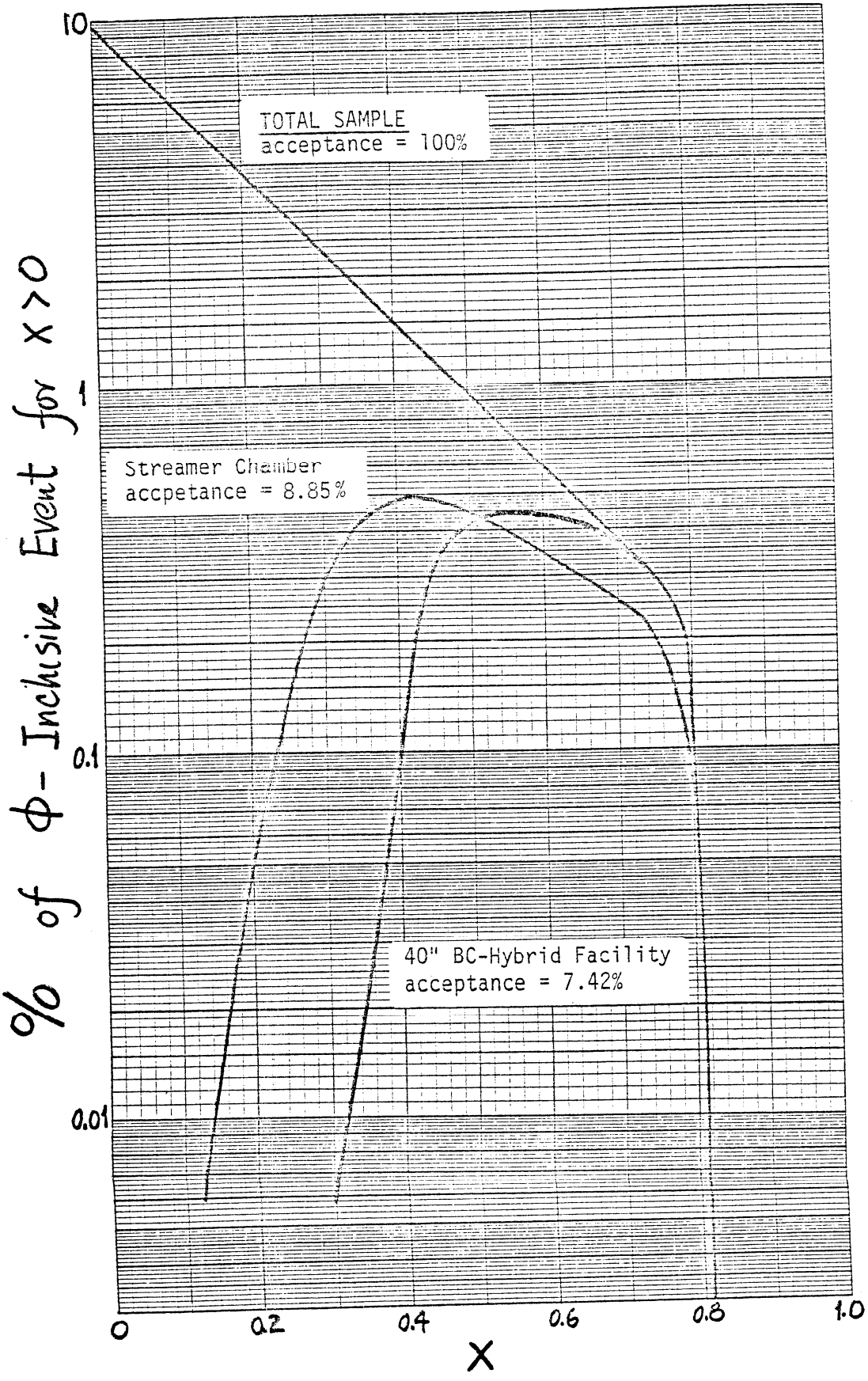
10
1
0.1
0.01
% of φ- Inclusive Event for x>0
TOTAL SAMPLE
acceptance = 100%
Streamer Chamber
accpetance = 8.85%
40" BC-Hybrid Facility
acceptance = 7.42%
0
0.2
0.4
0.6
0.8
1.0
X

E 131 Memo 1
Z. Ming Ma
January 7, 1977.

THE EXPECTED YIELD IN RELATIONS TO THE ČERENKOV COUNTER INEFFICIENCIES

In the proposal E 131, we have estimated our physics sample yield assuming that the Čerenkov counters will have a pion rejection efficiency of 99.9%. Careful studies of reported evaluations of other similar counters operating under similar conditions have convinced us that such a level of efficiency is indeed attainable. However, to anticipate the unexpected, we examine in this memo, the effects of Čerenkov counter inefficiencies on the expected physics sample.

I. Using an Unbiased 4π Detector

Figure 1 shows the expected mass spectra in this experiment. The top curve represents the entire K^- inclusive sample produced with the requested π^+ flux. Had such an ideal detector been in existence that can tag every K^- track in an event, the requested flux will produce a total of 7.37×10^5 events of the type

$$\pi^+ p \rightarrow K^+ K^- + X \qquad (1)$$

which has a cross section of 0.290 mb as is estimated in Appendix I of the proposal. In addition, there will be 2.29×10^5 events due to ϕ inclusive production

$$\pi^+ p \rightarrow \phi + X \qquad (2)$$
$$\phi \rightarrow K^+ K^-$$

for a $\sigma \cdot B$ of 90μb as is estimated in Appendix II of the proposal. The ϕ signal in this curve assumes a Gaussian full width, 2β of 10 MeV/c^2. A Monte Carlo study using a spatial resolution of 360 μm and the ϕ production characteristics as is discussed in Appendix II, indicates[1] a Gaussian full width of 4 MeV/c^2. Nevertheless, we use 10 MeV/c^2 as a conservative estimate in this memo. If one takes every event with a K^- track, regardless of whether the associated strange particle is a K^o or a K^+, the mass spectrum

for $K^- X^+$ is represented by the top curve in Figure 1. Here X^+ stands for a positive track interpreted as a K^+. There are 5.08×10^6 combinations. At the center of the ϕ-signal, the signal to noise ratio is expected to be 8 to 1.

Since such an ideal 4π detector does not exist, one looks to the next best choice - a bubble chamber. Without a general particle identification capability[2], one has to deal with the problem of wrong interpretations due to the tremendously large π^- inclusive production. At 15 GeV/c, one has

$$\pi^-/K^- = 24.50\text{mb}/480\mu\text{b} = 51 \qquad (3)$$

Assuming that the mass spectrum due to $\pi^- X^+$ where π^- is interpreted as a K^- is similar to that of the K^-X^+ spectrum, we expect that the signal to noise ratio will become

$$(8/1) \times (1/51) = 1/6.4 \qquad (4)$$

At this level, one will not be able to extract the ϕ signal from the background without cuts.

II. Using the K^- Trigger Logic

The middle curve in Figure 1 depicts the expected mass spectrum in this proposal assuming no π^- contamination. The ϕ signal (10.1 K events) stands over the K^-X^+ background (1.79×10^5 combinations) in a ratio of 16 to 1 at the center of the ϕ mass. This represents a twofold improvement of the signal to noise ratio over the case with an "ideal 4π detector."

At a mass of 1.8 GeV/c^2, the differential cross section is given by

$$\frac{d\sigma}{dM} = 3.4 \times 10^4 / 2.54 = 1.34 \times 10^4 \text{ nb/10 MeV/}c^2$$

As is indicated by the middle curve in Figure 1, one expects $\sim 1.3 \times 10^3$ mass combinations per 10 MeV/c^2 bin. Therefore, to search for the production of a ϕ' state with a 3 standard deviation effect, in a 10 MeV/c^2 bin, one needs

$$\sigma \cdot B \geq 3\sqrt{1.3 \times 10^3} \times 1.34 \times 10^4 / 1.3 \times 10^3 = 370 \text{ nb} \qquad (5)$$

Now, suppose the pion rejection efficiency is only 99.5%, the question is what effect does this have on the viability of this experiment?

As we have discussed in Section III(b) of the proposal, a 10^{-3} inefficiency will introduce a 25% contamination into that K^- sample. Therefore, a 5×10^{-3} inefficiency will result in a 125% π^- contamination. In the region of the ϕ signal, we expect the signal to noise ratio be reduced from 16 to 1 to 7 to 1. For the ϕ' search, the $\sigma.B$ sensitivity is reduced to 560 nb for a 3 standard deviation effect. We believe with even a 5×10^{-3} pion rejection efficiency, this experiment is still very viable. The principle problem will be the larger film measuring load. We expect to have

$$1.01 \times 10^4 + 2.25 \times (2.43 \times 10^4 + 1.59 \times 10^4) = 1.01 \times 10^5 \text{ triads} \qquad (6)$$

This is a significant measurement load, but not an overwhelming one.

At this point, it is useful to check our estimates against the unpublished results from the Omega Spectrometer at CERN. The experimental setup is shown in Figure 2. An unseparated negative beam impinges upon a 60 cm liquid hydrogen target. Outgoing charged particles are detected by the optical spark chambers. There are eight modules along the beam direction and four in the transverse direction. These chambers are placed in a large 1.8T superconducting magnet. Downstream of the spark chamber is a large aperture, atmospheric pressure isobutane Čerenkov counter sandwiched in between two planes of scintillation hodoscopes. The isobutane Čerenkov counter has a pion rejection inefficiency[3] of $\sim 2\text{-}3 \times 10^{-3}$. Figure A.II.1a of the proposal shows the weighted mass spectrum of K^-"K^+" combinations. The data are from a 16 GeV/c

$$\pi^- p \to K^- + X \qquad (7)$$

run. From a total of 5.9×10^5 good triggers, $\sim$2200 ϕ events were recorded. Correcting for geometric acceptance, the experiment yielded

~5200 weighted ϕ events. The invariant mass distribution of the trigger K^- tracks with all available positive candidates interpreted as a K^+ is shown in Figure A.II.1a of the proposal. A clear ϕ signal stands above a sizable background. For $1.016 < m < 1.06$ GeV/c^2, the signal to noise ratio is 0.64 to 1. At 18.5 GeV/c, the π^- inclusive cross section[4] for π^-p interaction is 50.8 ± 1.1 mb as compared with 26.7 ± 1.0 mb for π^+p interactions. The total inclusive cross section for π^-p is a factor of two higher than for π^+p and the ratio is highly x-dependent. For example, at 18.5 GeV/c, the ratio of invariant cross sections in x varies from 1.56 at x=0 to ~80 at x=1. Therefore, for a similar level of Čerenkov counter pion rejection inefficiency, the background contamination is likely to be much more serious for the trigger reaction (7) than in the case of a π^+ beam. Thus not knowing the exact geometry of the Omega Spectrometer and the details of the trigger logic, we can only say that the worse ϕ signal to noise ratio in that experiment is consistent qualitatively with known facts.

III. Using K^-K^+ Trigger with $P_{x^+} > 2.55$ GeV/c

In this section, we discussed the fall-back positions available if for some unforeseen reason, the π^- contamination in our experiment is much higher than we have expected. As has been discussed in the proposal, our Monte Carlo study indicates that for the ϕ inclusive sample triggered by the K^- logic, almost all of the associated K^+ tracks are contained in a spot 1 m high by 1.4 m wide at 3 m downstream of the target. Detailed studies using a six-cell isobutane Čerenkov counter, similar to that in the K^- arm indicate that the ϕ signal can be enhanced by requiring that the positive charged track entering the K^+ Čerenkov counter satisfy the following criteria:

(1) no Čerenkov counter in the appropriate cell as is determined by extrapolating the candidate track from the streamer chamber

through the PWC planes in front and behind the V Cerenkov counter,

(2) the laboratory momentum be greater than 2.55 GeV/c, the threshold momentum for a π^+ track.

The probability that a pair of pions fakes both V Cerenkov counters is given by the product of the pion rejection inefficiencies of the two counters. Therefore using the K^+ tagging information, we can reduce pion background substantially. The expected K^-K^+ mass spectrum is shown by the lower curve in Figure 1. At the center of the ϕ mass the signal to noise ratio is 51 to 1. The improvement of the signal to noise ratio is primarily attributable to the elimination of π^+ contaminations. Using this technique, we will be able to obtain a sample of 6300 ϕ events as compared with 10100 ϕ's as we have proposed.

The sensitivity for a ϕ'search is reduced to $\sigma.B \geq 2.3$ μb for a 3 standard deviations enhancement if the resonance has a width of 10 MeV/c^2. At this level, we feel our experiment to search for a ϕ'state is no longer competitive. However, this proposal will allow us to study ϕ production mechanism at a level of 63 event/μb. This is a factor of 3 greater than the next best experiment done thus far.

REFERENCE

[1]For formula relevant for this estimate, see F. Villa, SLAC-PUB-1250 (1973).

[2]Monte Carlo studies indicate that only 10% of the K^- tracks are expected to be below 1 GeV/c, where track ionization density may be useful in mass identifications using a bubble chamber.

[3]P. Sonderegger, private communication, September 11, 1976.

[4]J.T. Powers et.al, Phys. Rev. D8, 1947, (1973).

FIGURE 1

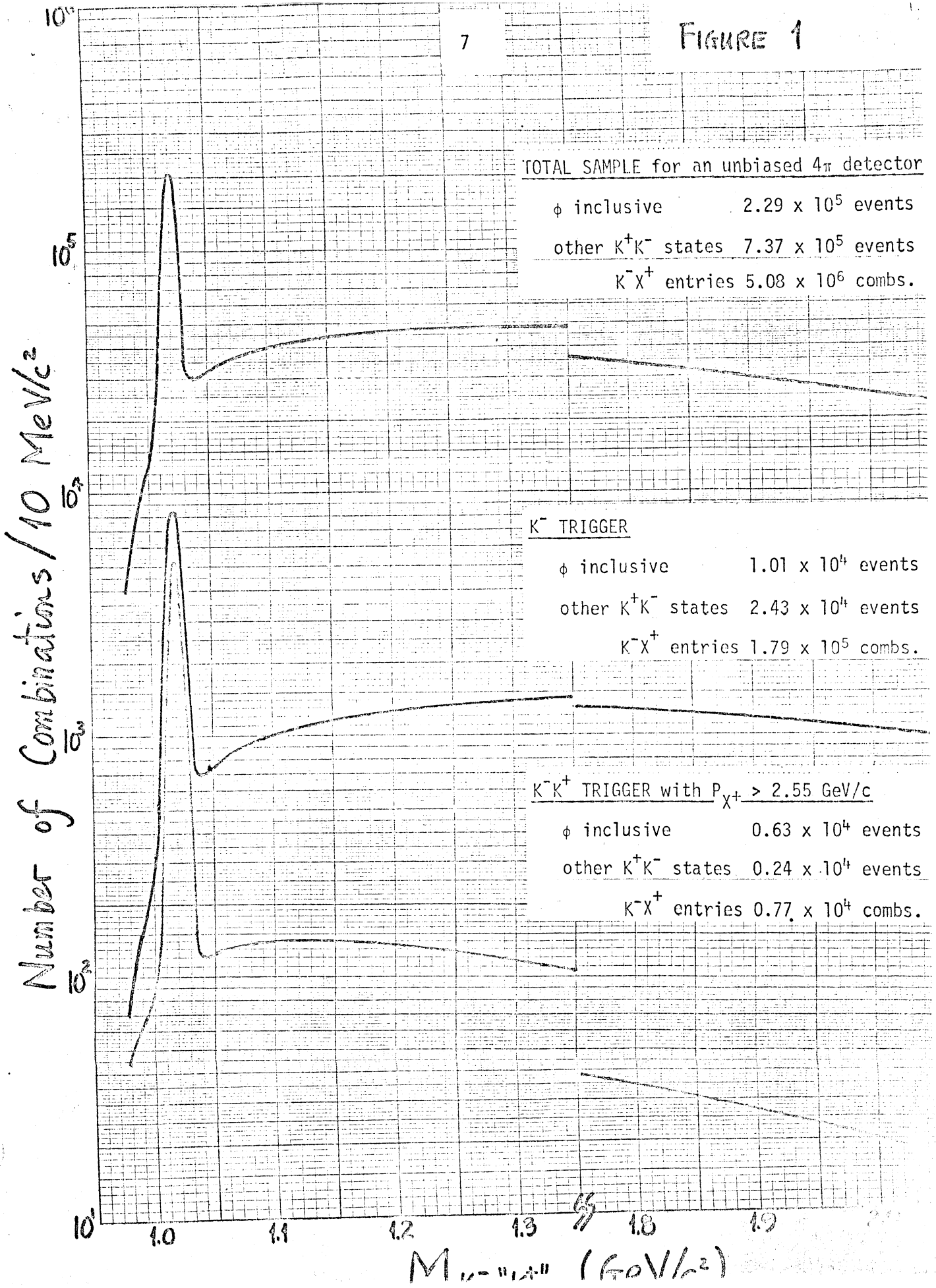
TOTAL SAMPLE for an unbiased 4π detector
φ inclusive 2.29 x 10^5 events
other K+K- states 7.37 x 10^5 events
K-X+ entries 5.08 x 10^6 combs.
K- TRIGGER
φ inclusive 1.01 x 10^4 events
other K+K- states 2.43 x 10^4 events
K-X+ entries 1.79 x 10^5 combs.
K-K+ TRIGGER with P_X+ > 2.55 GeV/c
φ inclusive 0.63 x 10^4 events
other K+K- states 0.24 x 10^4 events
K-X+ entries 0.77 x 10^4 combs.
Number of Combinations / 10 MeV/c²
10^5
10^4
10^3
10^2
10^1
1.0
1.1
1.2
1.3
1.8
1.9
M (GeV/c²)

FIGURE 2

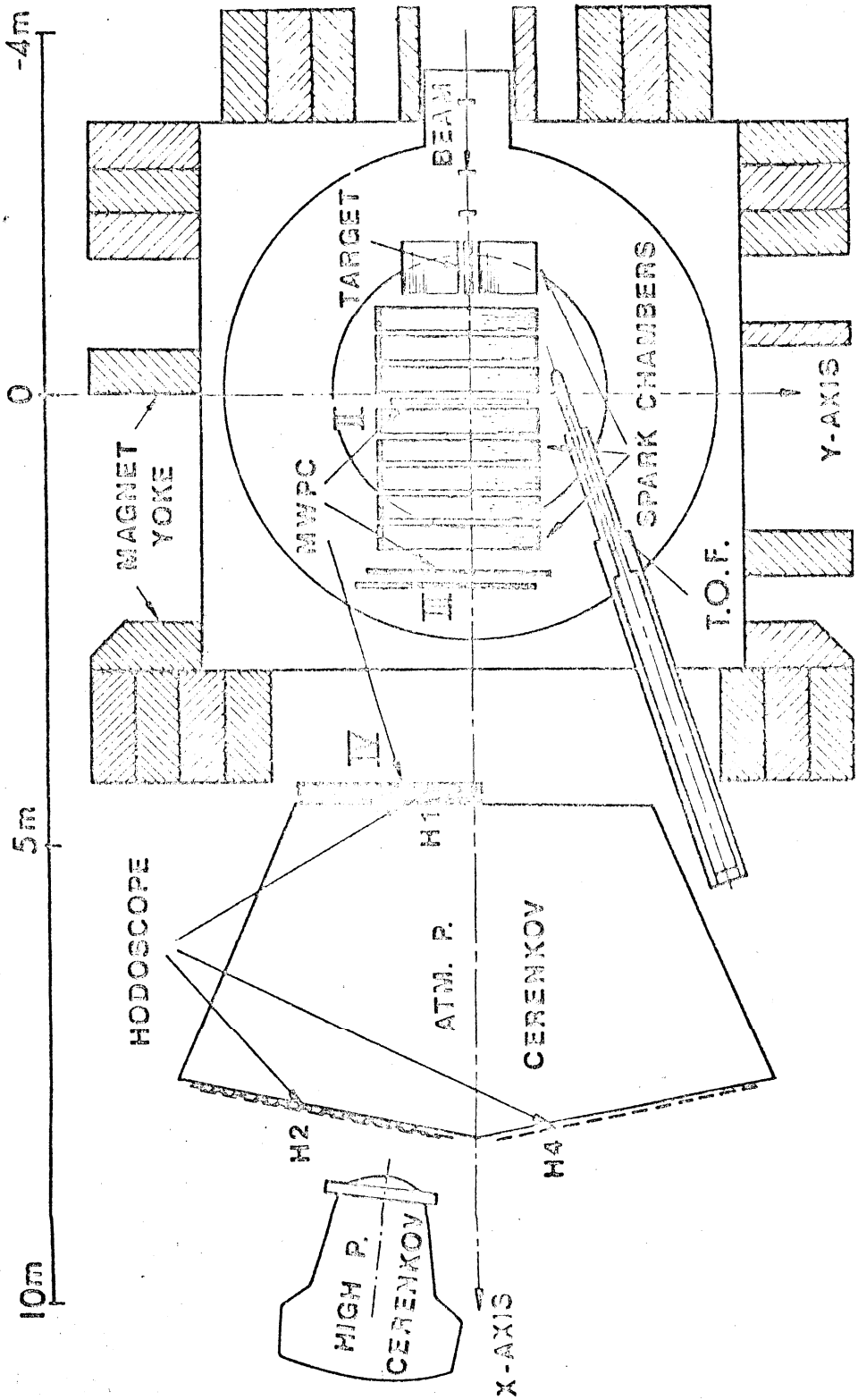
-4m
0
5m
10m
BEAM
TARGET
MWPC
MAGNET YOKE
SPARK CHAMBERS
T.O.F.
Y-AXIS
X-AXIS
H1
H2
H4
HODOSCOPE
ATM. P.
CERENKOV
HIGH P. CERENKOV

E 131 Memo 2
J. Hylen, V. Whitelaw
and Z. Ming Ma
January 21, 1977

LIGHT COLLECTION CONSIDERATIONS FOR A TEN-CELL ATMOSPHERIC PRESSURE ISOBUTANE CERENKOV COUNTER

This counter is designed to veto π^- which have satisfied the picket fence logic. The logic limits the π^- momentum to the isobutane threshold of 2.55 GeV/c and above.

The counter has 2 rows of 5 mirrors each. Each column of two mirrors is placed so that it will detect the light produced by a set of four scintillation counters. To take account of the photon spread from one cell to the next, each fourth counter straddles two mirrors, and its trigger is vetoed by a signal from either cell. The dimensions and orientations of the mirrors are given in Table 1. The layout of the Cerenkov counter is shown in figure 1.

In this study, the π^- are produced according to experimental distributions by Monte Carlo methods, and those which satisfy the hodoscope logic are tracked through the Cerenkov counter. The Cerenkov photons are generated at an angle θ_c with respect to the π^- and are reflected by the mirror system to the collecting Winston light funnels, one for each mirror. The Cerenkov angle is given by

$$\cos \theta_c = \frac{1}{\beta n} \qquad (1)$$

where β is the velocity of the π^- and n is the index of refraction of the isobutane gas used in the counter. The Cerenkov angle spectrum of the π^- accepted by the picket fence logic is shown in figure 2.

The amount of light produced depends on the momentum, and is proportional to $\sin^2\theta_c$. The average path length between emitting photons is given by

$$< L > \doteq (A \times \sin^2\theta_c)^{-1} \qquad (2)$$

where the parameter A characterizes the spectrum of the expected Cerenkov light, the wavelength dependence of the photomultiplier tube responce and quantum efficiency. Corrected for the transmission losses through the atmospheric isobutane, a value of A = 218 photoelectrons/cm is used. This corresponds to the Amperex 58 UVP tube. A 20% increase is expected for RCA 4522. The distance between successive photon emission along the π^- path is generated according to the distribution $_e$-L/<L>.

A radius of 2 m for the mirrors is chosen to give a focus at the Winston funnel entrance 1 m from the center of the mirror. A space of 1/2 cm is left between adjacent mirrors to allow some leeway for final adjustment, and the Monte Carlo takes into account losses in these cracks. The mirror widths and positions have been adjusted individually to maximize the collection efficiency for photons produced by the π^-.

Using a total of 5392 π^- that satisfy the picket fence logic, we observed that the photons reflected from each mirror form a spot at the collection plane with an maximum diameter of 18 cm and a maximum entrance angle to the cone of $\pm 26^o$. These can be accommodated by a 38.7 cm long Winston funnel[1] with a 26.2 cm diameter opening at one end reducing gradually down to a 11.5 cm diameter for a 5" phototube. The geometric light collection efficiency for photons produced by the triggering pions is shown in figure 3. The average efficiency is 96.8%.

Other losses are now considered. The photon intensity is further reduced by the reflectances of the mirror (assumed to be 85%) and the Winston funnel wall (also 85). To better match the wavelength spectrum of the Cerenkov photons and the phototube window, a wavelength shifter, paraterphenyl (pTP) will be coated on the entrance window of the phototube. Published studies[2] indicate that the pulse height from a pTP coated phototube is about 95% of that from a phototube with a UV transmitting quartz window. Folding in all three losses, the Cerenkov photon intensity is expected to be reduced to 70% of the initial intensity.

Finally, the acceptance curve was broadened by Poisson statistics.

Figure 4 shows the final number of accepted photoelectrons per triggering π^-. If we assume a pulse height requirement of 2 to 5 p.e. for a positive discriminator signal, the counter inefficiency against triggering π^- ranges from 4×10^{-4} to 6×10^{-4}. The largest part of this inefficiency is due to π^- which are barely above threshold, and could be removed by either an off-line momentum cut on the triggering particle, or an off-line examination of the phototube pulse height.

In summary, we have completed a photon collection study for the 10-cell isobutane Cerenkov counter. Using π^- generated according experimental data and the picket fence logic requirement, the produced Cerenkov photons are ray-traced through the proposed optical system. Taking into account all known causes for photon losses, the expected inefficiency against π^- is expected to be between 4 and 6×10^{-4}.

REFERENCE

1. H. Hinterberger and R. Winston, Rev. Sci. Inst. 37, 1094 (1966).

2. E. L. Garwin, Y. Tomkiewicz and D. Trines, Nucl. Inst. and Methods 107, 365 (1973).

Table 1 - DIMENSIONS AND ORIENTATIONS OF THE MIRROR SYSTEM*

Mirror Number	Tilt Angle About X	Tilt Angle About Y	Center of Mirror X	Y	Z	Width ΔX	Height ΔY
1,6	±.262	.03	- .21	±.33	6.	.415	.655
2,7	"	.07	- .605	"	"	.365	"
3,8	"	.08	- .97	"	"	.355	"
4,9	"	.09	-1.325	"	"	.345	"
5,10	"	.13	-1.75	"	"	.495	"

* 10 Mirrors in 2 rows of 5 each, each with a radius of 2 m.

Angles in radians, distances in meters.

A space of 1/2 cm is allowed between mirrors.

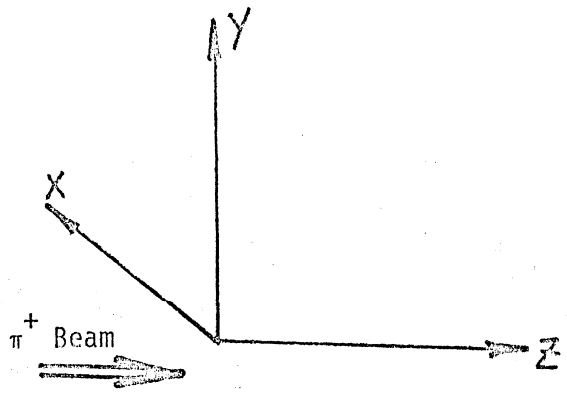

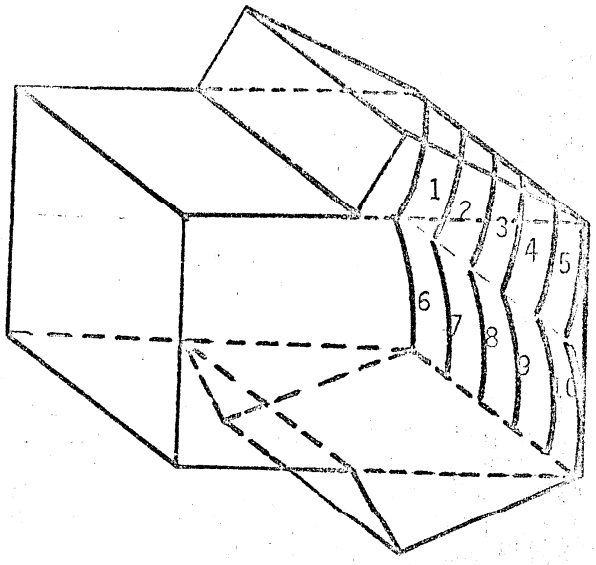

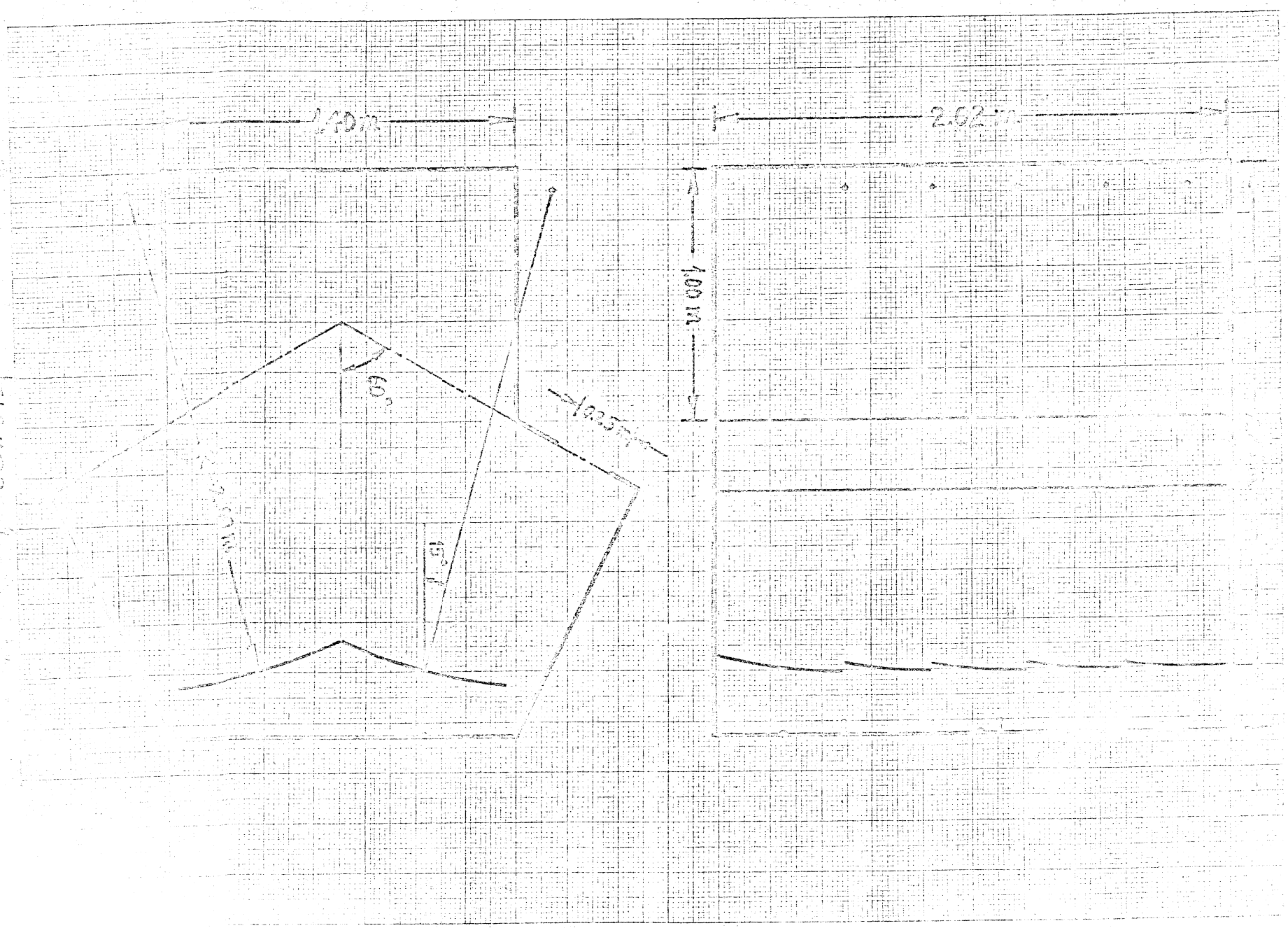

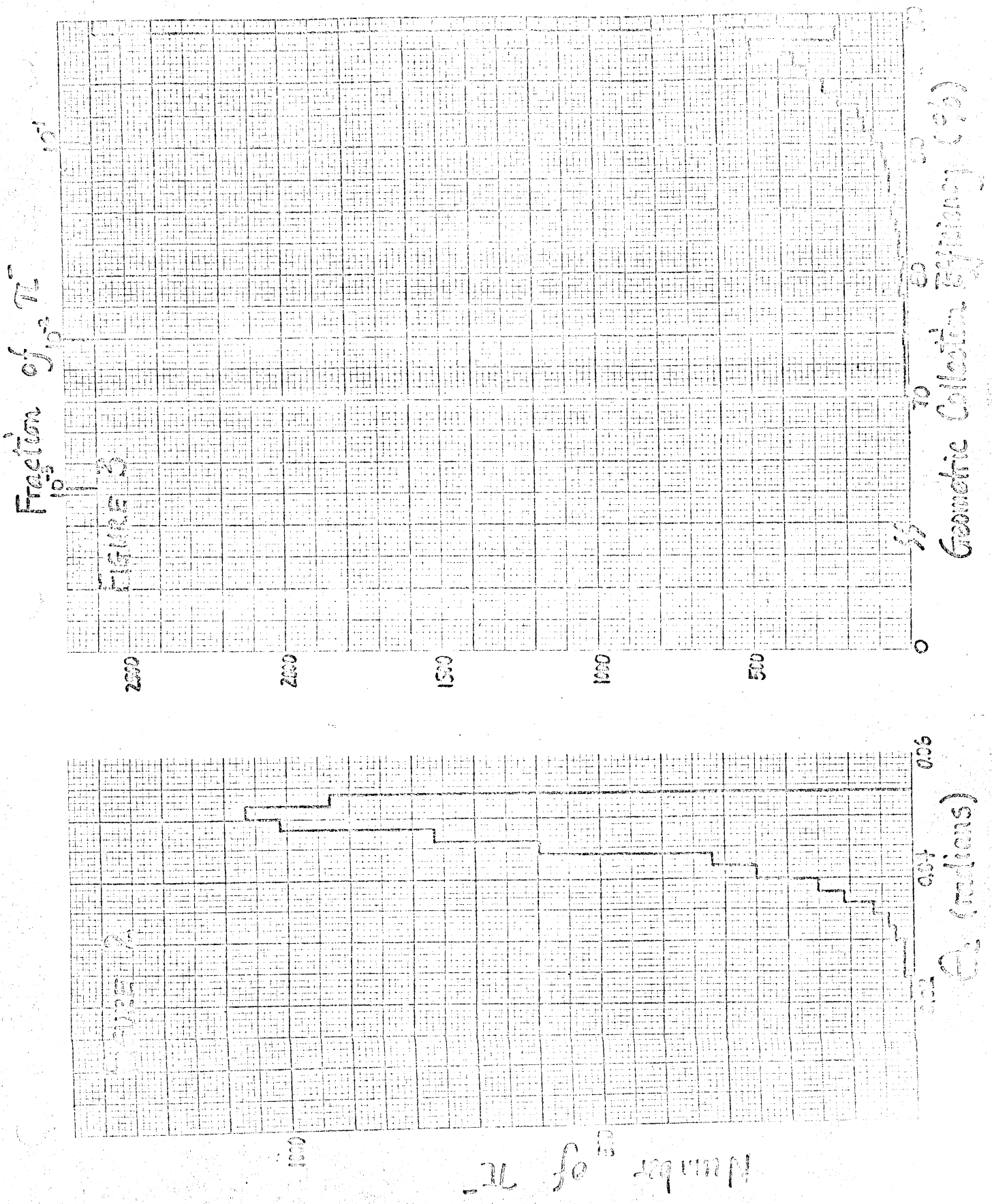
Fraction of π^-
Geometric Collection Efficiency (%)
Number of π^-
π^- Energy (MeV)

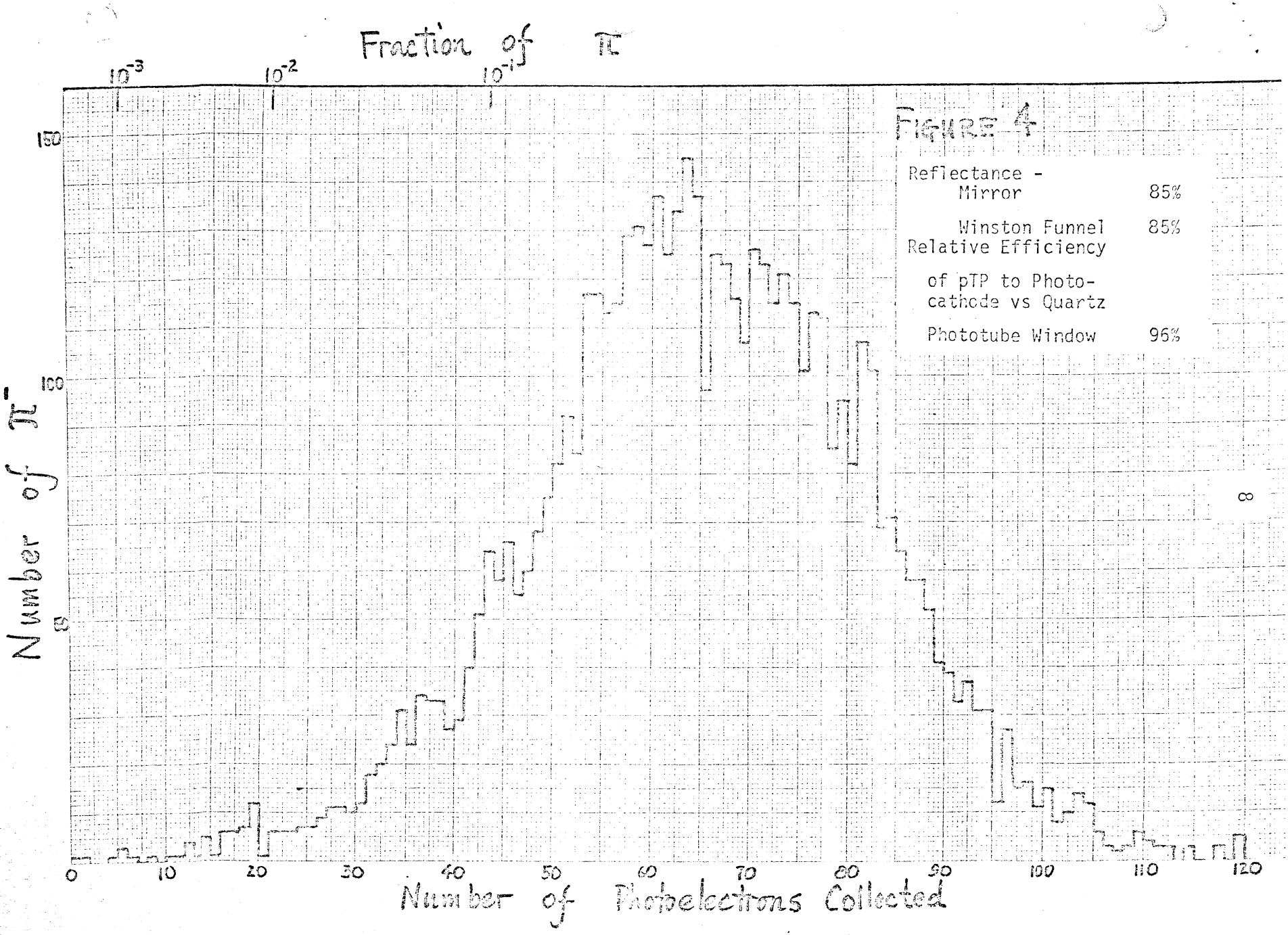
Fraction of π
10^{-3}
10^{-2}
10^{-1}
FIGURE 4
Reflectance - Mirror 85%
Winston Funnel Relative Efficiency of pTP to Photocathode vs Quartz 85%
Phototube Window 96%
Number of π⁻
150
100
50
0
10
20
30
40
50
60
70
80
90
100
110
120
Number of Photoelectrons Collected